THE UNIVERSITY OF MICHIGAN

INDUSTRY PROGRAM OF THE COLLEGE OF ENGINEERING

FLUID-DYNAMIC PERFORMANCE OF A CAVITATING VENTURI

F. G. Hammitt
C. L. Wakamo
P. T. Chu
V. E. Cramer

October, 1960

IP-472

ACKNOWLEDGMENTS

The authors wish to acknowledge the financial support of the NASA in the investigations herein reported.

Personnel having a major part in these studies, aside from the authors, were: Wm. Beckman, Edwin Flanigen, Siman Perez, Jonathon E. Schmidt, John Summers, Arthur Travers, and Wm. Walsh. In addition, great assistance in design and fabrication of the equipment was received from Mr. Edward Rupke, supervisor of the Instrument Shop, The University of Michigan Research Institute.

TABLE OF CONTENTS

LIST OF FIGURES

LIST OF FIGURES
(Continued)

1.0 INTRODUCTION

As a flow measuring or metering device, a cavitating venturi meter is of great utility in certain cases because the flow is a significant function only of the upstream pressure. As long as it is operated only over that flow range where cavitation is well established, a change in downstream pressure results only in an extension or dimunition of the cavitating region. The flow is controlled almost entirely by the pressure differential between upstream pressure and the pressure at which cavitation is initiated--approximately the vapor pressure of the fluid. Hence, as long as fluid temperature is constant the flow rate is quite closely a function only of the upstream pressure. In its general behavior the cavitating venturi is very similar to a DeLaval nozzle over that range of conditions where sonic velocity is attained in the throat; the region of collapse of the cavitation vapor bubbles is analogous to the normal shock wave which may exist in the nozzle. Qualitative descriptions of the flow phenomena are provided in References 1, 2, 3, and 4.

Unfortunately these handy and simple relations are not entirely realized in practice, partially because cavitation is not initiated precisely at the vapor pressure of the fluid, but rather at a pressure which may depend upon absolute system dimensions, fluid velocity, type of fluid, fluid purity, temperature (aside from the simple vapor pressure effect), gassification of the fluid, pressure-time relations, etc., and partially

because of non-homogeneity of vapor-mixture liquid, non-uniformity of velocity profile, and other secondary effects. The existence and importance of the various effects in the first category have been the subjects of numerour recent research investigations in the cavitation field. References 5 through 12 are cited as examples, References 5, 6, and 7 providing good summaries of the literature in this regard. It is the purpose of this report and a second report which will follow at a later date, to present additional semi-quantitative observations and measurements of the flow in such a system.

Cavitating venturis, in addition to their application as flow metering and measuring devices have received considerable attention as research tools for the study of cavitation in general. As is well known, a better understanding of the effects of cavitation both with respect to fluid-dynamic performance and to the damaging of materials is vital to continued progress in the development of high-performance, light-weight, and economicla fluid-handling machinery components. For research purposes, cavitation can be produced in actual machines (or scale models thereof). However, this is not always the most advantageous procedure because of the imperfect knowledge of the fluid-flow pattern in such machines, even in the absence of cavitation, and because of the expense and difficulty of achieving suitable instrumentation, especially in cases where the fluids to be studied present handling difficulties (nonambient temperature, toxicity, corrosiveness, etc.).

An alternative to the use of actual flow machines for the study of cavitation, is the production of cavitation in a static system using sonic and ultra-sonic techniques as, for example, the electrical driving

of a piezo-electric crystal immersed in the fluid. In general, cavitation can be produced in this manner with a minimum of mechanical complications and expense. However, with the present state of knowledge of the phenomenon, there is doubt regarding the direct application of results so achieved to the actual fluid machinery problems.

For many purposes, the cavitating venturi offers an optimum compromise. It involves a system which is reasonably uncomplicated mechanically so that the handling of different fluids becomes feasible. There exists a good understanding of the flow patterns, at least in the absence of cavitation and precise instrumentation can be achieved easily. In addition, the system is a flowing system with the possibility of obtaining pressure gradients similar to those which exist in an actual machine, so that the application of results is reasonably direct.

The present investigation has been undertaken with the objective of studying performance and damage effects of cavitation in a system capable of handling various fluids of interest at non-ambient temperature levels, (as liquid metals and cryogenic fluids) and yet one simulating conditions which are close enough to those existing in machinery components of interest to allow a direct application to be made. Pursuant to this objective, it was first necessary to investigate quantitatively the cavitating behavior of the system using ordinary water as the test fluid. The results of this investigation form the content of this report and of a second report which will follow in the near future. The present report deals primarily with measurements and observations describing the flow pattern itself. The

second report will cover measurements of pressures and cavitation numbers for different degrees of cavitation, fluid velocities, temperatures, degrees of aereation, test section size, etc.

2.0 General Description of Flow

It has long been recognized[1,2,3,4] that the flow pattern in the cavitating region of a cavitating venturi diffuser is characterized by a jet, more or less completely liquid, surrounded by a more or less vaporous region. A photograph of such flow in a two-dimensional diffuser[1] has been reproduced in this report (Figure 1). Detailed measurements are largely lacking, and it is hoped that the data herein will aid in filling this gap.

The lowest pressure of the system occurs at the entrance to the diffuser, owing to the frictional losses in the throat. If the streamlines were to follow the walls at the diffuser entrance, a radial pressure gradient toward the walls would be required. This is impossible if the pressure at the diffuser entrance is close to the vapor pressure, so that separation of the streamlines from the walls occurs at this point, giving the central free jet flow pattern. However in a certain axial region in the diffuser, depending upon the pressure maintained at the diffuser discharge, the vaporous region terminates and is replaced by a complete liquid flow. However, Figures 8, 9, 18, 19, and 25 all indicate that this termaination is not sharply defined. This region of termaination may be considered as analogous to a hydraulic jump, if it is considered that the change in static pressure across the region is analogous to the change in level height across the jump. In other words, presumably there is a standing

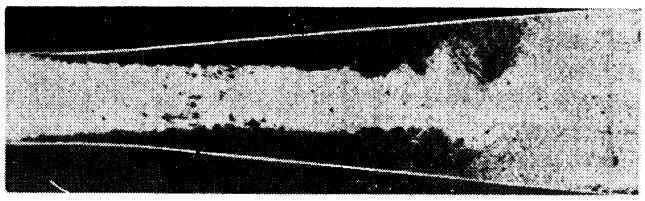

Figure 1. Flow in A Cavitating Venturi

wave with a velocity relative to the upstream medium equal to that of an hydraulic jump, wherein the change of level across the jump is numerically equal, in consistent units, to the change in static pressure across the collapse region in the diffuser. Calculations of this sort have been reported[2,3] where it is assumed that there is a liquid jet in the diffuser of uniform velocity equal to the throat velocity, and hence of the throat diameter, surrounded by a void space. The void collapses abruptly, and liquid of uniform velocity fills the diffuser. It is found that agreement between the velocities so calculated and the measured pressures exists only if a suitable coefficient is applied.

Several methods were utilized in the work herein reported to verify the existence of approximately such a flow pattern in the conical venturi-diffuser used, and to attempt to obtain more detailed information on this pattern. The approaches used were as follows:

a) Velocity measurements using micro-Pitot tube

b) "Void fraction" measurements using gamma-ray differential attenuation between vapor and liquid phases

c) High-speed motion pictures

The experiments were of a somewhat preliminary nature, and the utmost precision was not attained. However, valuable quantitative information regarding the nature of the phenomena in the cavitating venturi has resulted.

2.1 Description of Major Equipment Items

Two plexiglas venturis were used for the tests herein reported. (See Figures 2 and 3.) They were geometrically similar; i.e.: angles of convergence and divergence (approximately 6° included angle to prevent separation); and the ratios of cylindrical throat length to diameter were the same. However, there was a scale factor of about 7/4 between the units. The throat diameter of the larger was 0.503 inches; of the smaller, 0.287 inches. The overall lengths of the units were the same for mechanical reasons. This was accomplished by allowing a different cut-off diameter to the nozzle and diffuser portions between the units. However, this does not materially affect the fluid-dynamic similarity requirements because the cut-off diameter in either case is large enough that the kinetic head at this point is virtually negligible. Each venturi is equipped with pressure taps spaced along the length, the exact locations being indicated in the figures. The tap size was approximately 1/16 inches; great care was taken to smooth the points of entry into the venturi. Besides use for pressure measurement, these taps were used for the installation of an acoustic transducer. This, as well as pressure measurements results, will be explained in later reports.

The entire closed loop facility is shown schematically in Figure 4, while Figure 5* is an actual photograph. The facility, constructed of 1-1/2 inch, Schedule 40, stainless steel pipe, is powered by a

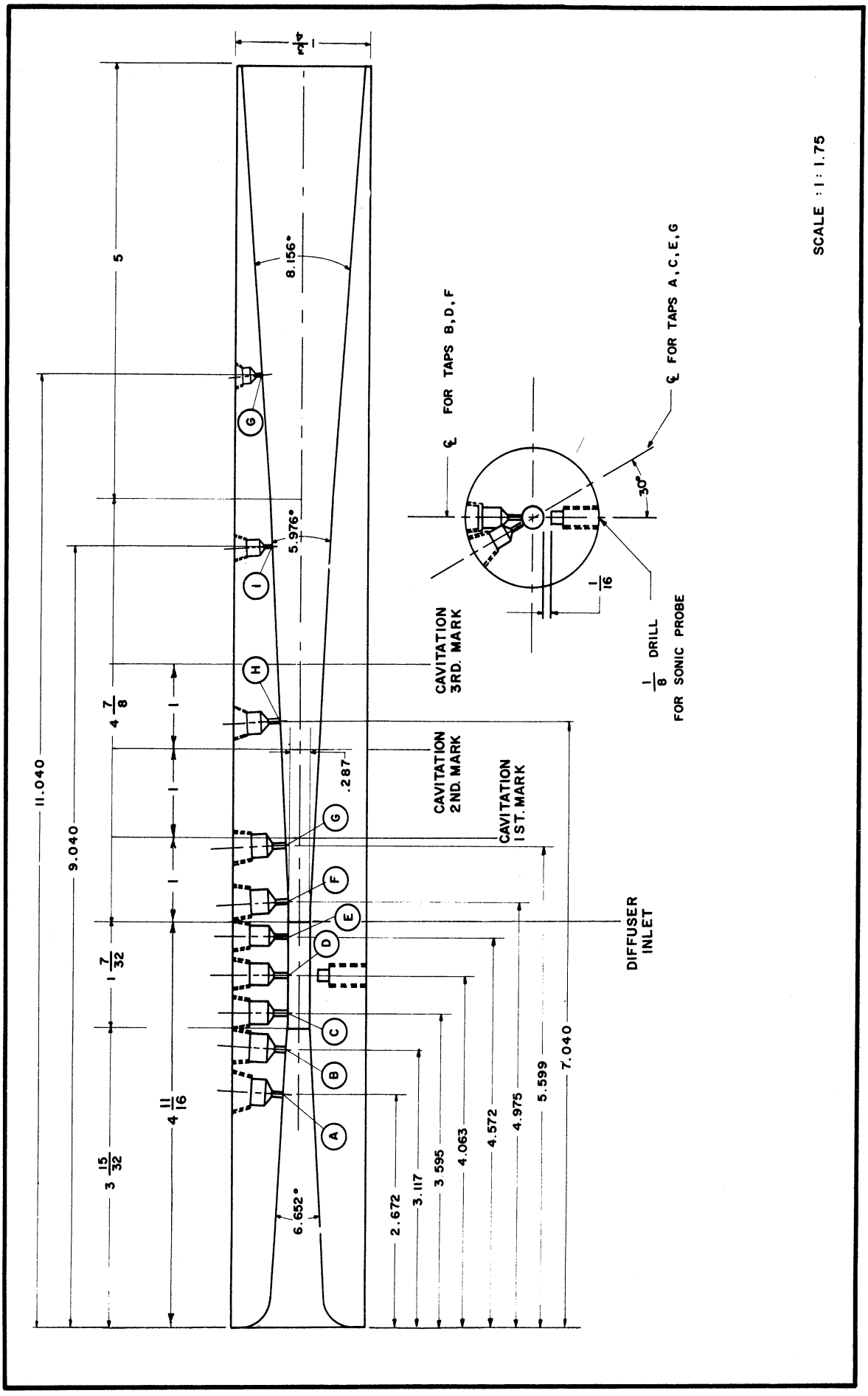

Figure 2. 1/4" Cavitating Venturi Test Section

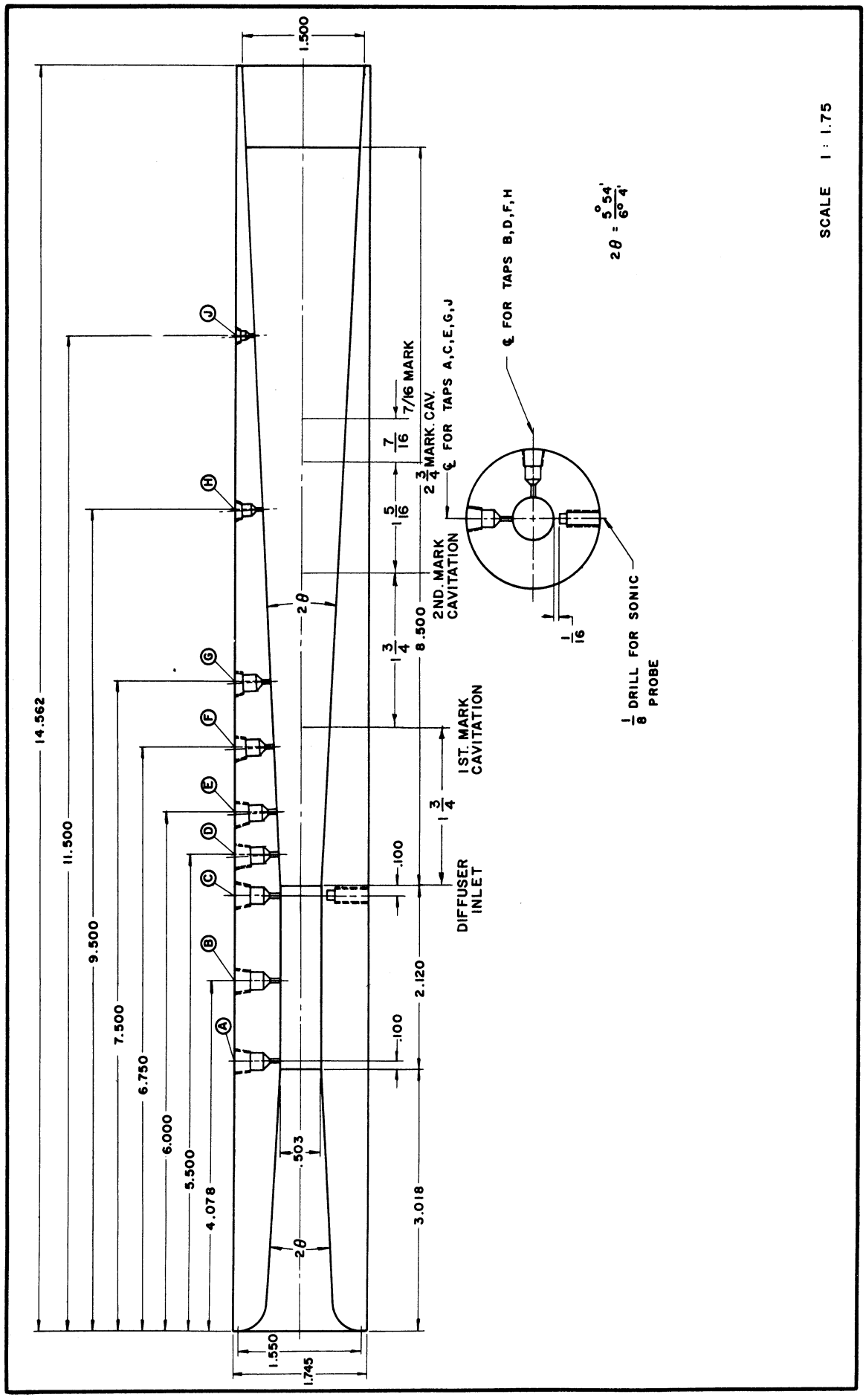

Figure 3. 1/2" Cavitating Venturi Test Section

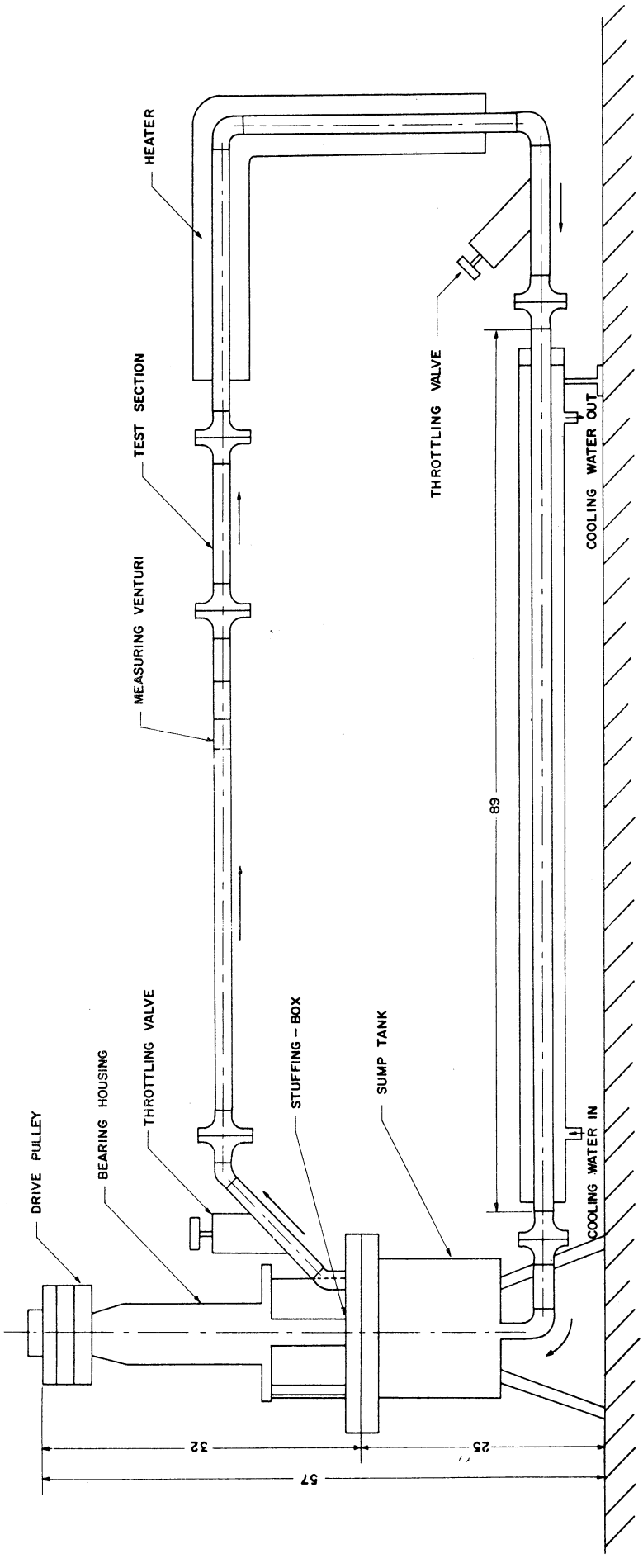

Figure 4. Sketch of Over-All Loop Layout

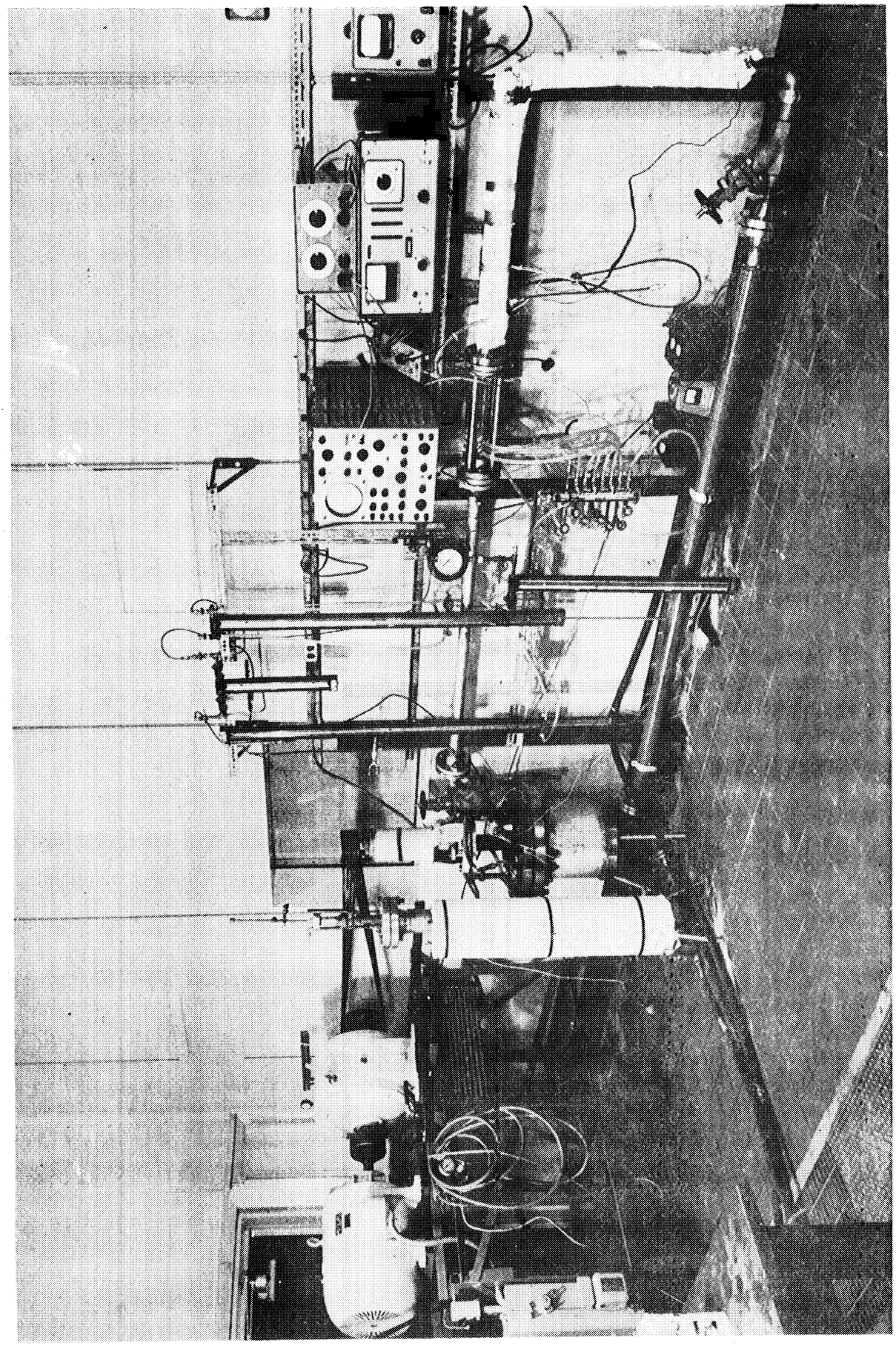

Figure 5. Photograph of Over-All Loop Layout

centrifugal "sump"-type pump, (i.e.: pump suction essentially exposed to atmospheric pressure), capable of producing a maximum cavitating velocity of about 95 feet per second in the throat of the larger venturi (mininum of about 50 feet per second under cavitating conditions as controlled by the necessity of diffusing back to atmospheric sump pressure), and somewhat more in the smaller venturi. Throttle valves are provided upstream and downstream of the venturi so that for a constant pump head and flow, venturi throat pressure can be adjusted. Flow is measured by a second calibrated venturi, and an electric resistance heater is provided on one of the piping legs. Further details of the loop are given in Reference 13.

A rough control of degree of aereation of the fluid is possible, even though contact with the atmosphere exists in the pump sump. This region is sealed along the pump shaft by a conventional stuffing-box which of course allows a small leakage rate. To prevent the excessive aereation which would occur if a substantial and agitated free surface were provided, the water level was maintained up to the stuffing-box, so that there was a continued out-leak at this point, necessary to cool the packing. Such an arrangement means a continual make-up, and hence dilution of the presumable deaereated system water.

Nevertheless, it was found possible to maintain the water with a total gas content on the order of 50 percent of saturation, at ambient temperature and one atmosphere as measured by a Van Slyke type apparatus. Deaeration could be achieved by sucking-off by vacuum pump the liquid-vapor mixture from the cavitating region in the venturi. The effectiveness of the process was

considerably increased by heating the water (the maximum was 160F approximately, because of the properties of the plexiglass venturi.). Alternatively, deaereated water could be produced outside the loop by maintaining heated water under vacuum (induced by conventional vacuum pump) in a five-gallon flask, and agitating periodically (loop capacity is about ten gallons). In some tests, the loop would be charged by deaereated water produced in this manner. Actually for most of the tests discussed in this report, it was attempted to maintain slightly deaereated water so that gross air entrainment would not interfere with results. More careful air-content control was exercised in the cavitation number tests which will be described in a future report.

2.2 Velocity-Probe Tests

2.2.1 General Objectives

Velocity-probe tests were undertaken to attempt to establish, rather roughly, the flow pattern existing in the cavitating venturi. It was anticipated that these tests would be used with other types of instrumentation to obtain as comprehensive a picture as possible, i.e., gamma-ray void fraction measurements, high speed motion pictures, and static wall pressure readings. It was felt that any or all of these techniques could be further refined if desired for additional, more precise tests.

2.2.2 Apparatus

The velocity-probe arrangements which could be used were severely restricted by the small diameter of the test section. For a first attempt, it was felt that a simple hypodermic needle, sized to fit the pressure-tap holes (1/16 inch) would suffice. A bigger instrument would block too

great a portion of the channel. A straight needle was used, with a 20.5 mil hole drilled normal to its axis in a flattened portion about 88 mils from the end of the needle (see Figure 6). Although it was realized that flow around the end of the needle would create unknown effects, it was felt that these would be proportionately small, and that the arrangement would suffice to obtain a close approximation of the velocity in the central jet, if such existed, and to delineate the edge of such a jet. It was realized that readings in the vaporous region surrounding the jet would be difficult to interpret because of the unknown density in this region, the presumed lack of homogeneity of the fluid, and the possibility of "condensation shocks" or "hydraulic jumps" analoguous to that discussed for the main cavitating region. These were actually observed, ahead of the needle (Figure 7).

Static pressure was taken to be that existing in the absence of the needle (when it was entirely withdrawn from the tube). It is realized that this is a further source of inaccuracy because the needle does block of the order of ten percent of the flow passage, denpending upon its axial location in the diffuser. In addition, the presence of the condensation shock around the needle changes the actual local static pressure, so that a conventional Pitot tube with static holes is required for better precision. However, this latter argument does not apply in the vicinity of the liquid jet, which was the region of major interest and the region passing most of the mass flow. The argument does help to explain the fact, which will be discussed later, that the apparent velocity does not fall off sharply on the edges of the presumed jet.

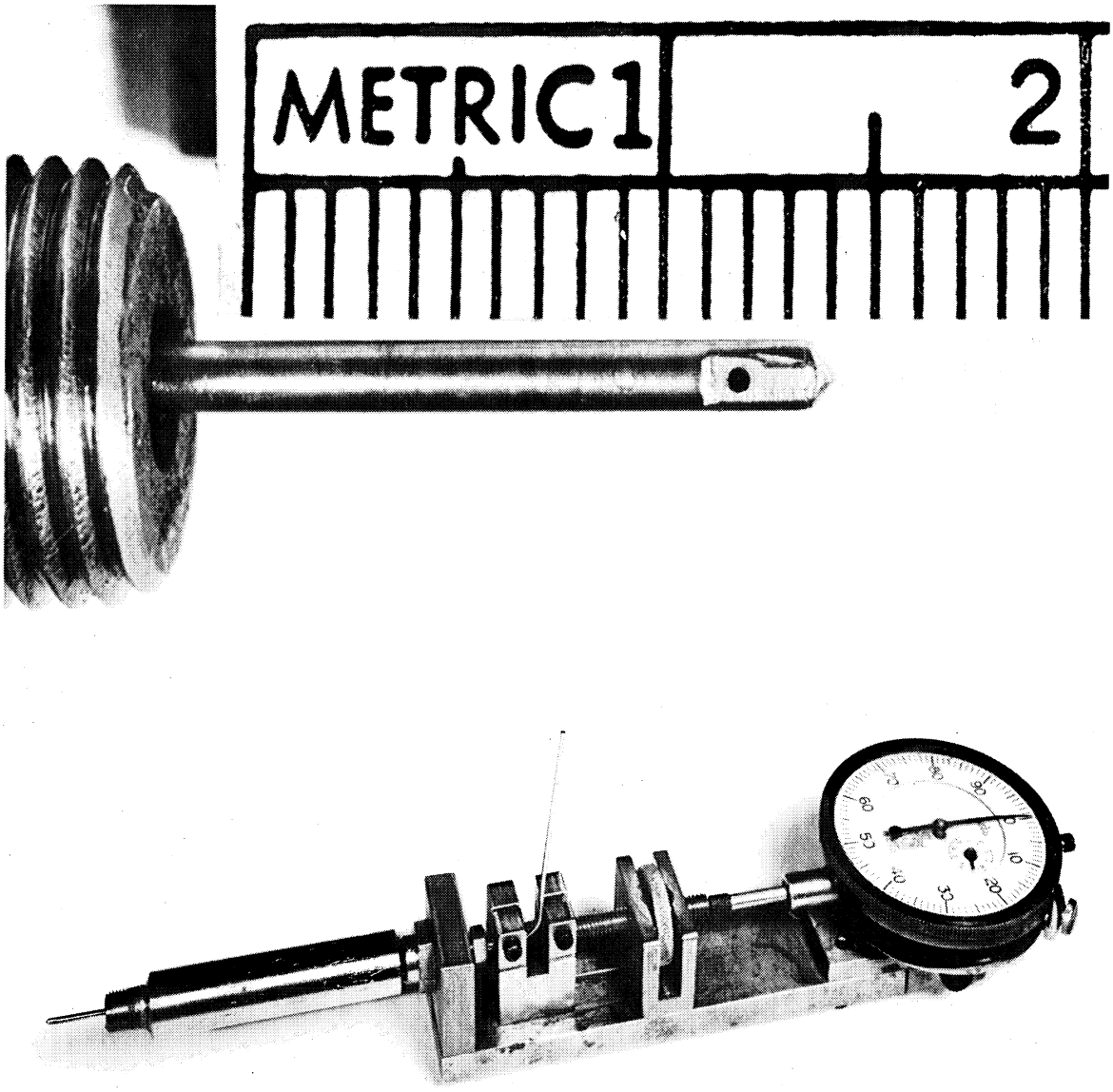

Figure 6. Micro Pitot-Tube

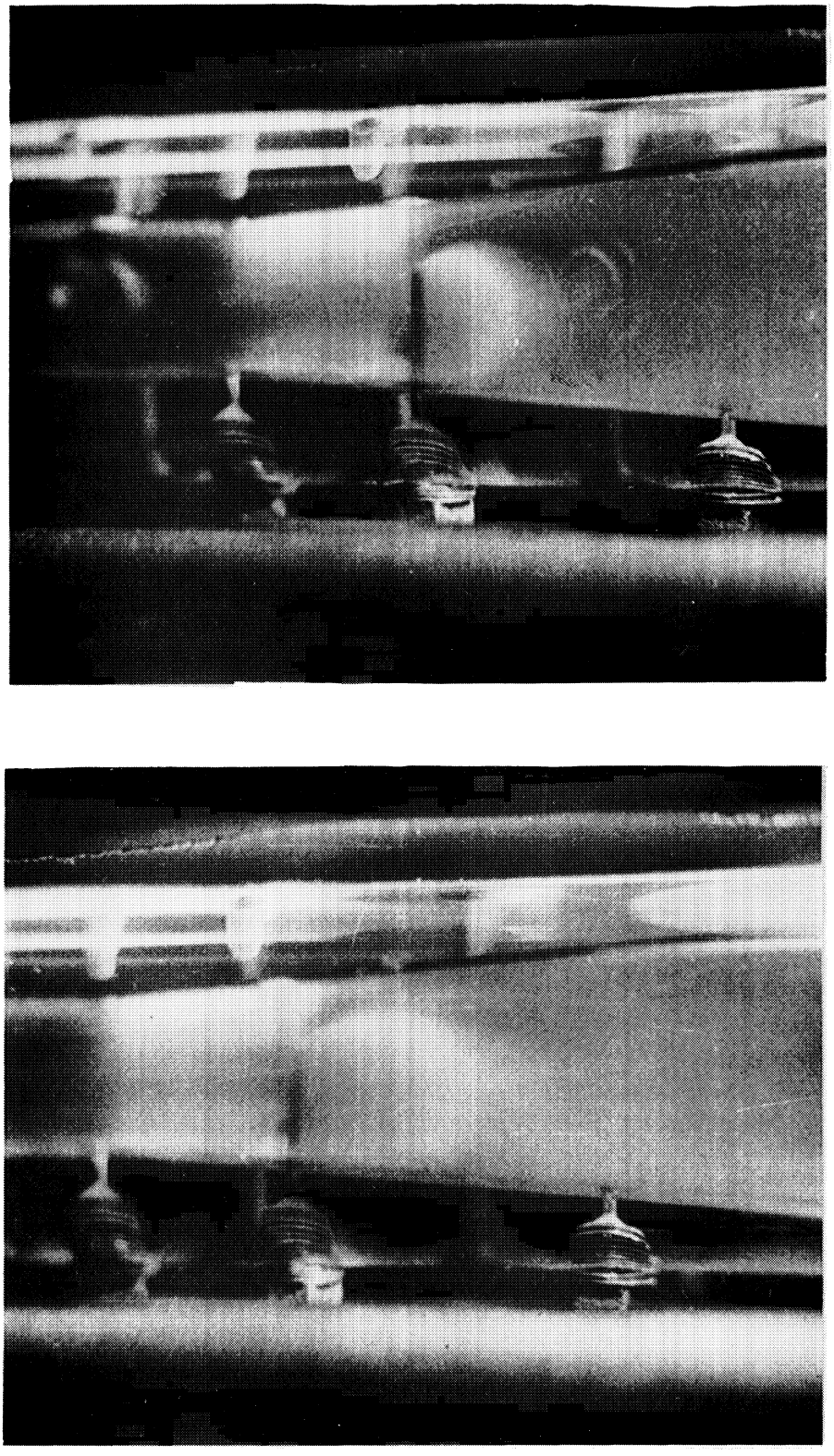

Figure 7. Photograph of Condensation Shock on a Needle

Radial motion of the needle was measured to the nearest mil, by an attached dial indicator. However, the point of entry into the stream could only be set by eye. It is felt that this setting was accurate to about five mils. The needle rotation could be adjusted manually to achieve the greatest impact head. It was found that such adjustment produced no measurable effect within about 10°, so that no important inaccuracies are encountered on this account.

2.2.3 Results of Measurements

2.2.3.1 General

In general, the measurements tend to confirm the presence of a central liquid jet in the cavitating region, which spreads in the approximate region of the visually-apparent termination of cavitation, to fill the entire cross-section. However, it appears that the radial location of the interface between vapor and liquid regions is not sharply defined, except perhaps near the throat. Likewise the axial location of the termination of the vaporous region is not sharp as with a normal shock wave, but rather spread over a fairly extensive axial region, which is of the order of about one inch with the venturi used.

If one considers a fixed axial location near the throat exit (say one - two inches downstream*), it is apparent that the existence and dimensions of the jet at this point is not affected by the extent of the cavitating region, as long as the collapse area is downstream of the

* Cavitation degree is indicated on all curves in terms of 1st Mark, 2nd Mark, etc. These indicate the axial location of cavitation termination as reference to the abscissas of the figures will show. For locations of marks see Figures 2 and 3.

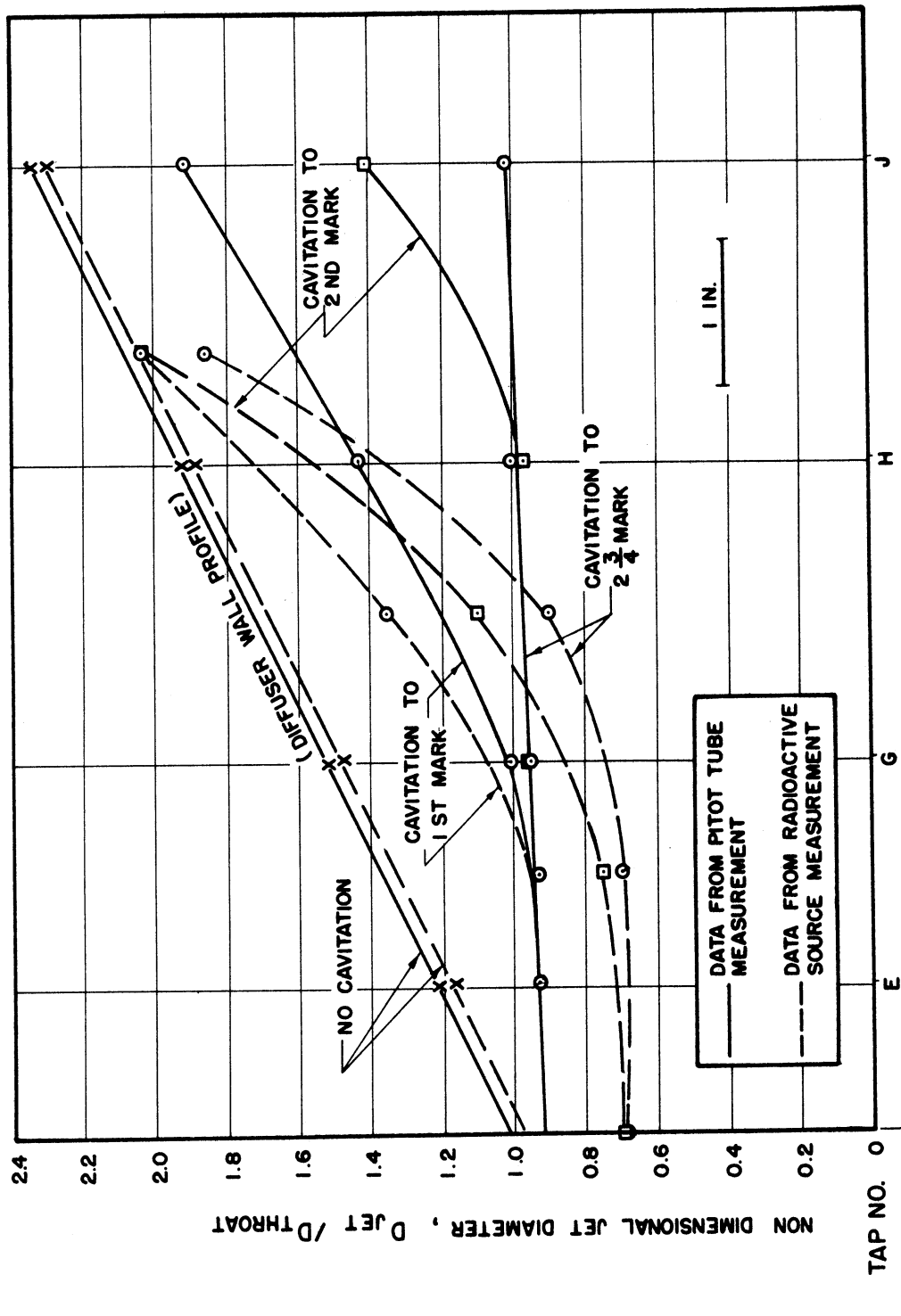

Figure 8. Non-Dimensional Liquid Jet Diameter as A Function of Axial and Cavitation Condition (Cold Water Data) 1/2 inch test section.

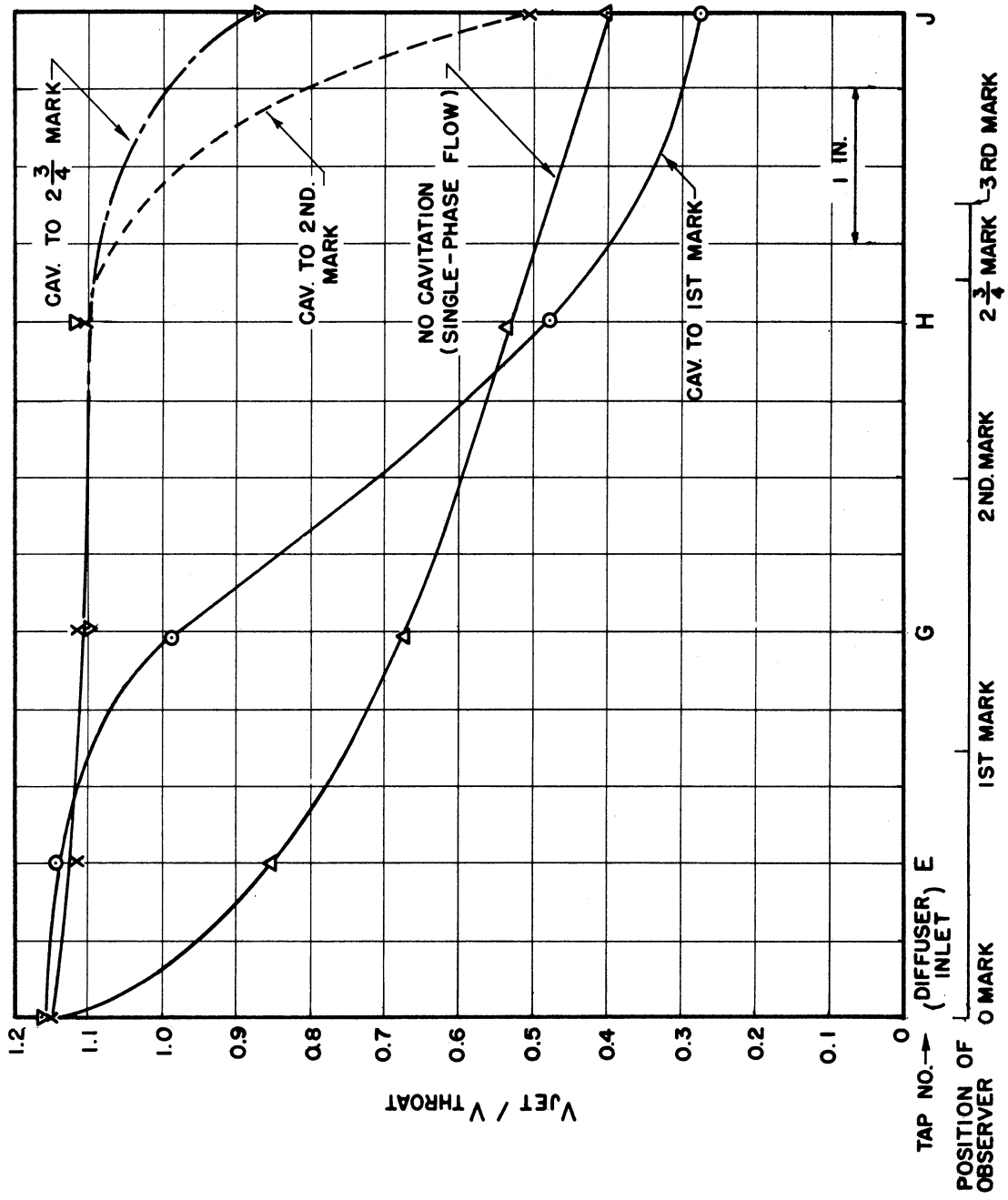

Figure 9. Mean Jet Velocity as Function of Axial Position and Cavitation Condition (Data by Pitot-Tube Method A), 1/2 inch Test Section

point of observation. This is shown by an examination of Figures 8 and 9 and is entirely consistent with the idea of a central jet. Also, at such a station it is noted that the jet velocity near the centerline is almost equal to the throat velocity, which is known from the measured flow rate and dimensions. Figure 9 shows a jet velocity at diffuser inlet up to 15 percent greater than the average throat velocity. This is partially a result of the fact that the Pitot tube blocks a varying portion of the flow area depending upon its degree of insertion whereas the throat velocity was computed for an unobstructed passage, partially of the fact that mean velocity is always less than the velocity near the centerline where the jet exists in this case, and partially of the inaccuracy of a Pitot tube of the type used. However, the data is sufficiently precise to show the major characteristics of the flow. At stations near the throat, the velocity profile is nearly flat over the extent of the jet, and is not a function of the extent of downstream cavitation (Figures 10 - 15). However, the velocity does not appear to fall off as sharply at the edges of the jet (which are known approximately from continuity calculations) as would be expected. As previously mentioned, this apparent fact may be the result of a "condensation shock" (Figure 7) in the region of the liquid vapor mixture which gives a considerably greater static pressure in the vicinity of the needle than that presumed from the wall static pressure measurements. Nevertheless, the existence of total pressures in the central portion of the test section which correspond to velocities nearly equal to the throat velocity can only be explained on the assumption of

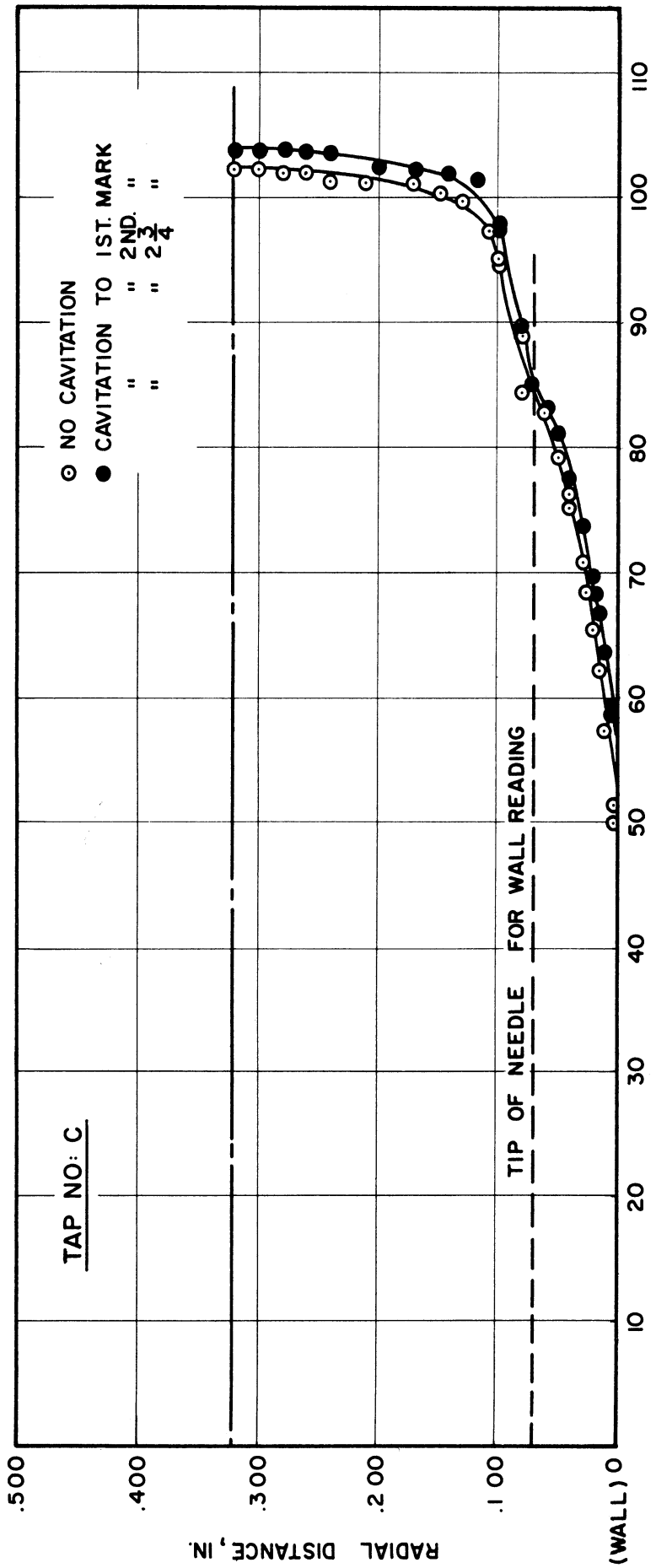

Figure 10. Velocity Profiles as Function of Radial Position and Caviation Condition, Observer at Tap Position C, Cold Water, 1/2 inch Test Section

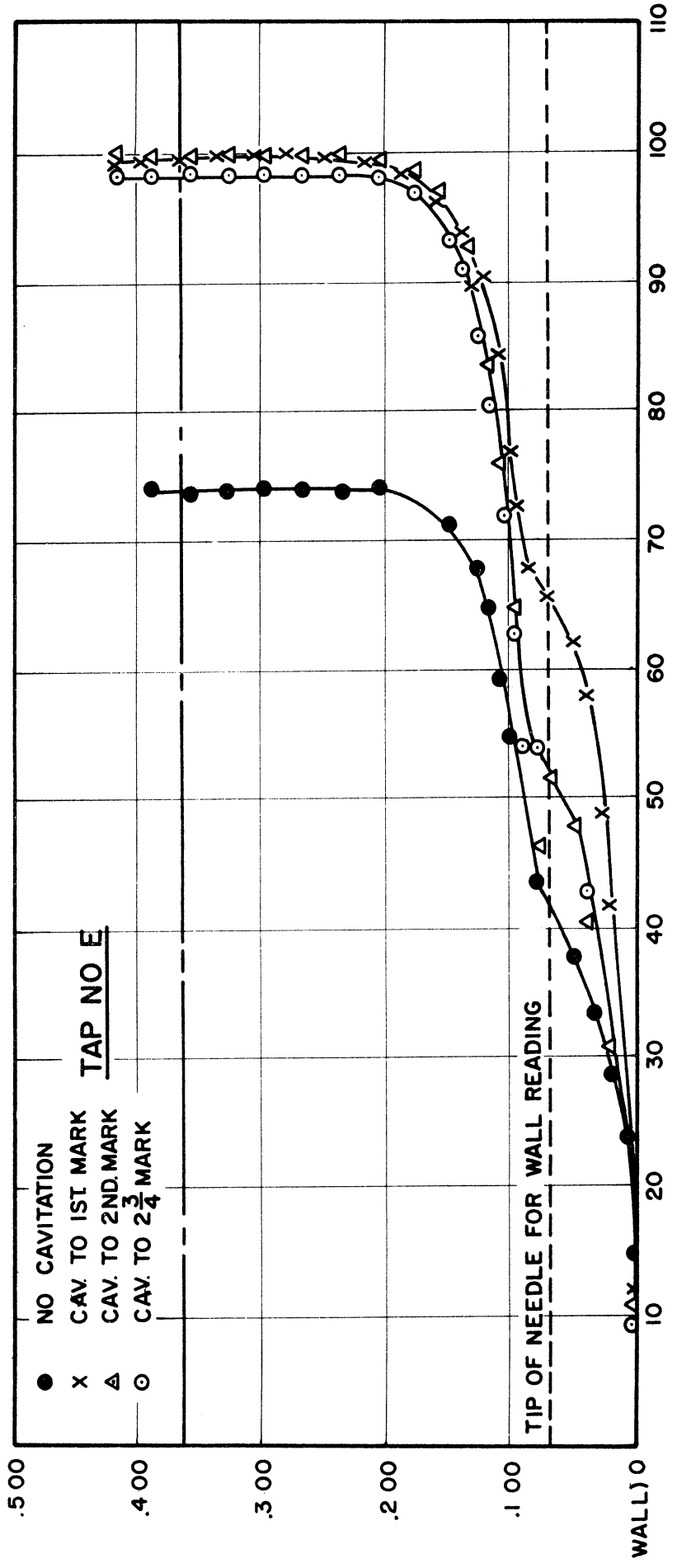

Figure 11. Velocity Profiles as a Function of Radial Position and Cavitation Condition, Observer at Tap Position E, Cold Water, 1/2 inch Test Section

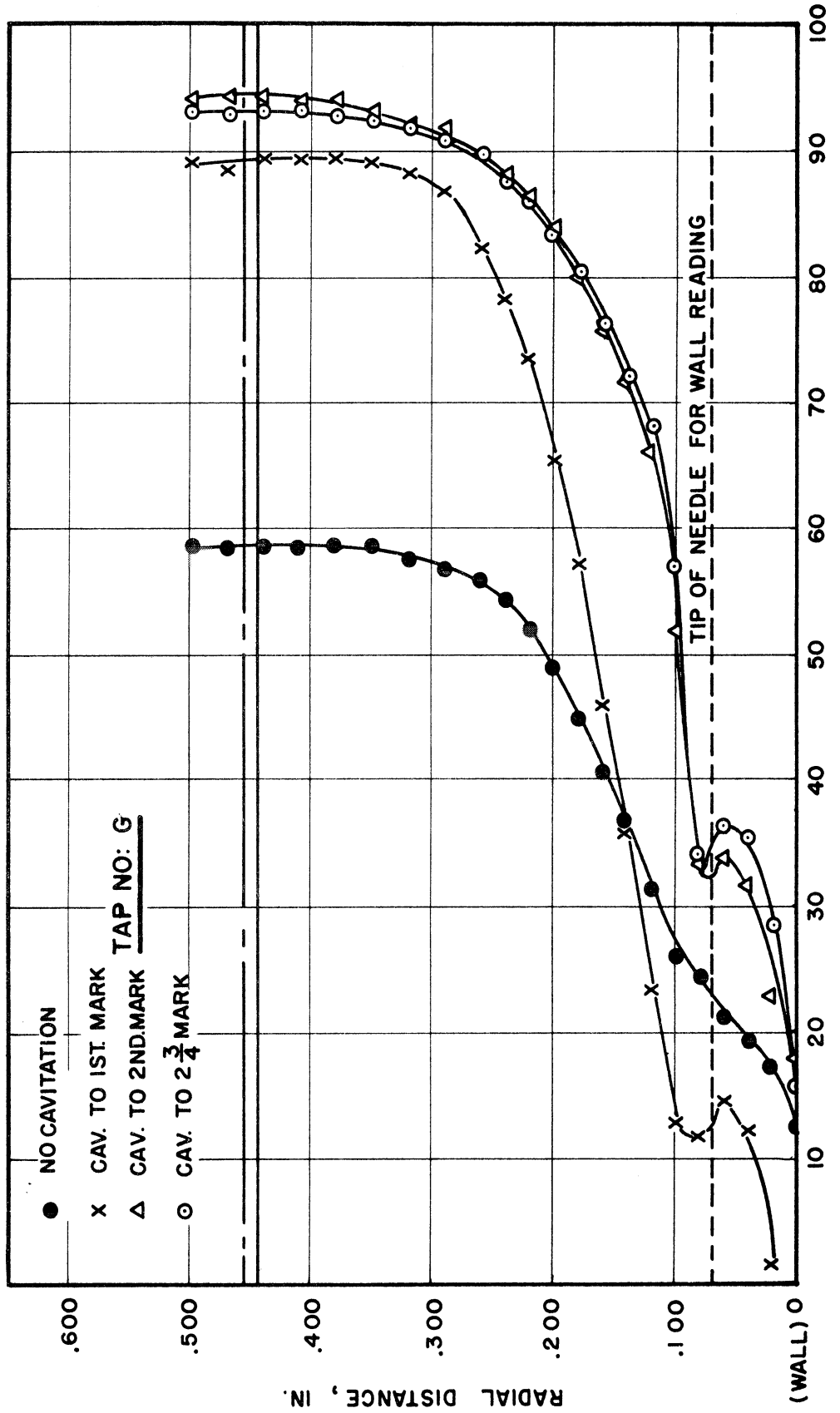

Figure 12. Velocity Profiles as Function of Radial Position and Cavitation Condition, Observer at Tap Position G, Cold Water, 1/2 inch Test Section

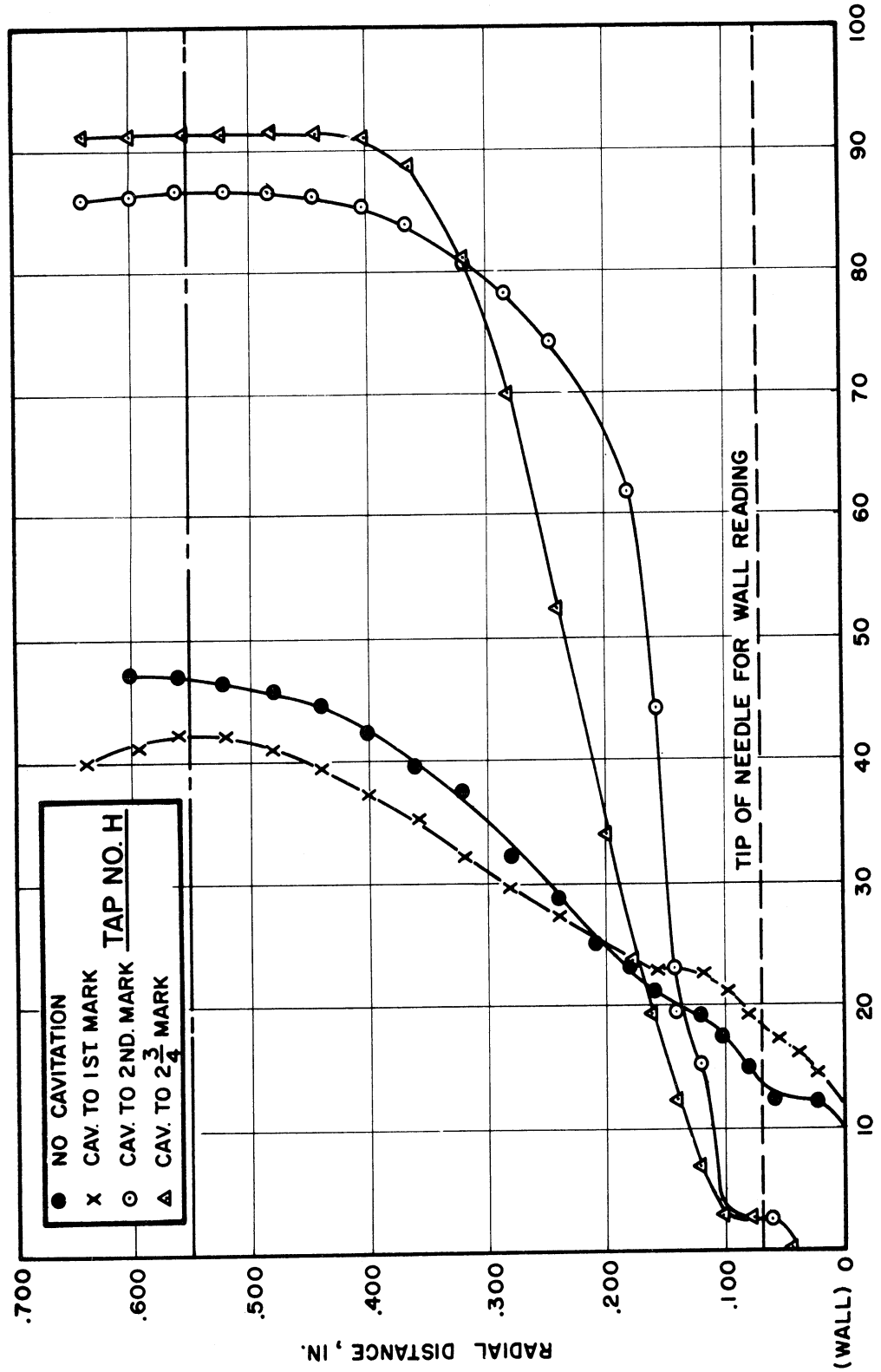

Figure 13. Velocity Profile as Function of Radial Position and Cavitation Condition, Observer at Tap Position H, Cold Water, 1/2 inch test section

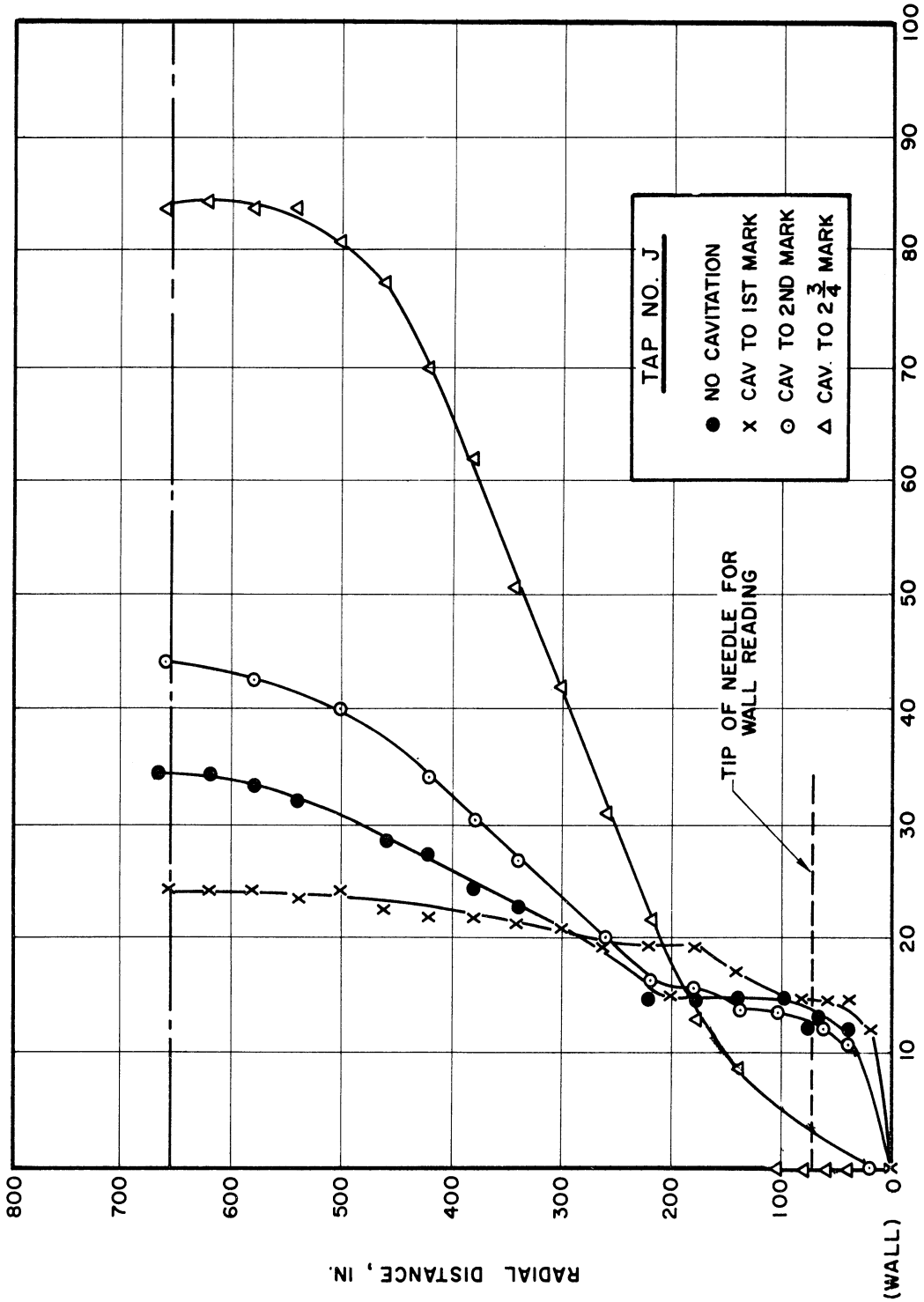

Figure 14. Velocity Profiles as Function of Radial Position and Cavitation Condition, Observer at Tap Position J, Cold Water, 1/2 inch test section

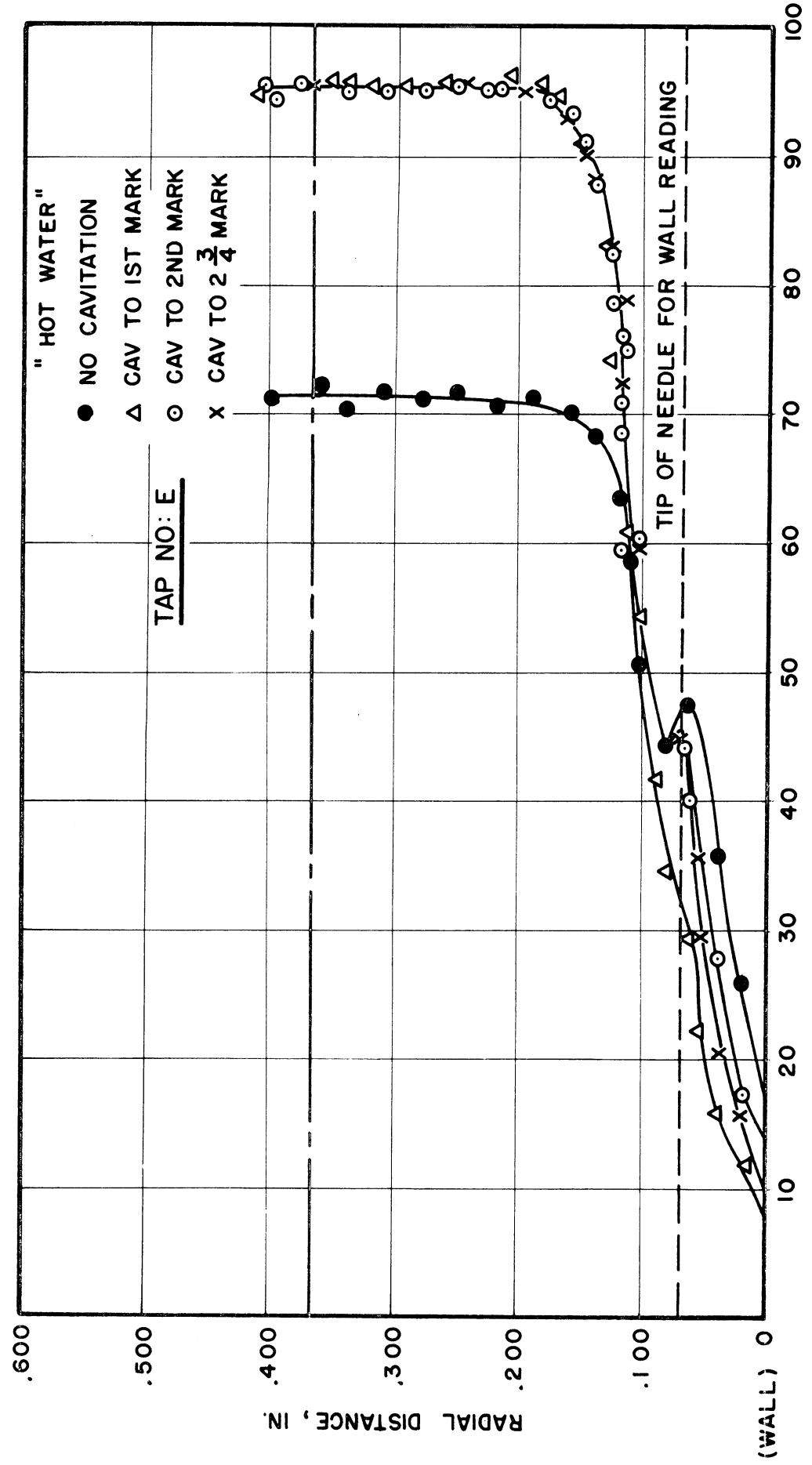

Figure 15. Velocity Profiles as Function of Radial Position and Cavitation Condition, Observer at Tap Position E, Hot Water, 1/2 inch Test Section

the actual existence of such velocities. If this is the case, continuity considerations, assuming attrition of the jet around the edges, limit the possible radial extent of such a jet to a radius slightly less than the throat radius.

The impact pressure measurements (reduced in alternate methods which will be discussed) and the void fraction measurements (described later) both show a jet diameter somewhat less than that of the throat diameter, as if a vena contracta existed. Considering the cylindrical nature of the throat section this seems somewhat surprising. However, it is further confirmed by the fact that the minimum static pressure for conditions of substantial cavitation is not in the throat but somewhat downstream. This comparison will be discussed in further detail in a future report.

As measurements are made for stations at increasing distance downstream from the throat, the radial velocity profile becomes more peaked toward the center, (Figures 10 - 15) but there still remains a portion of the cross section where the velocity is only slightly less than throat velocity, indicating that the central jet persists through most of the cavitating region, even when this extends several inches from the throat.

In general, for all stations, the extent of cavitation downstream from that station, so long as the cavitating region extends beyond the station, has little effect (Figures 8 and 9). Also, as mentioned, under any flow conditions, cavitating or not, the radial velocity profiles becomes less flat as the distance downstream from the throat is increased.

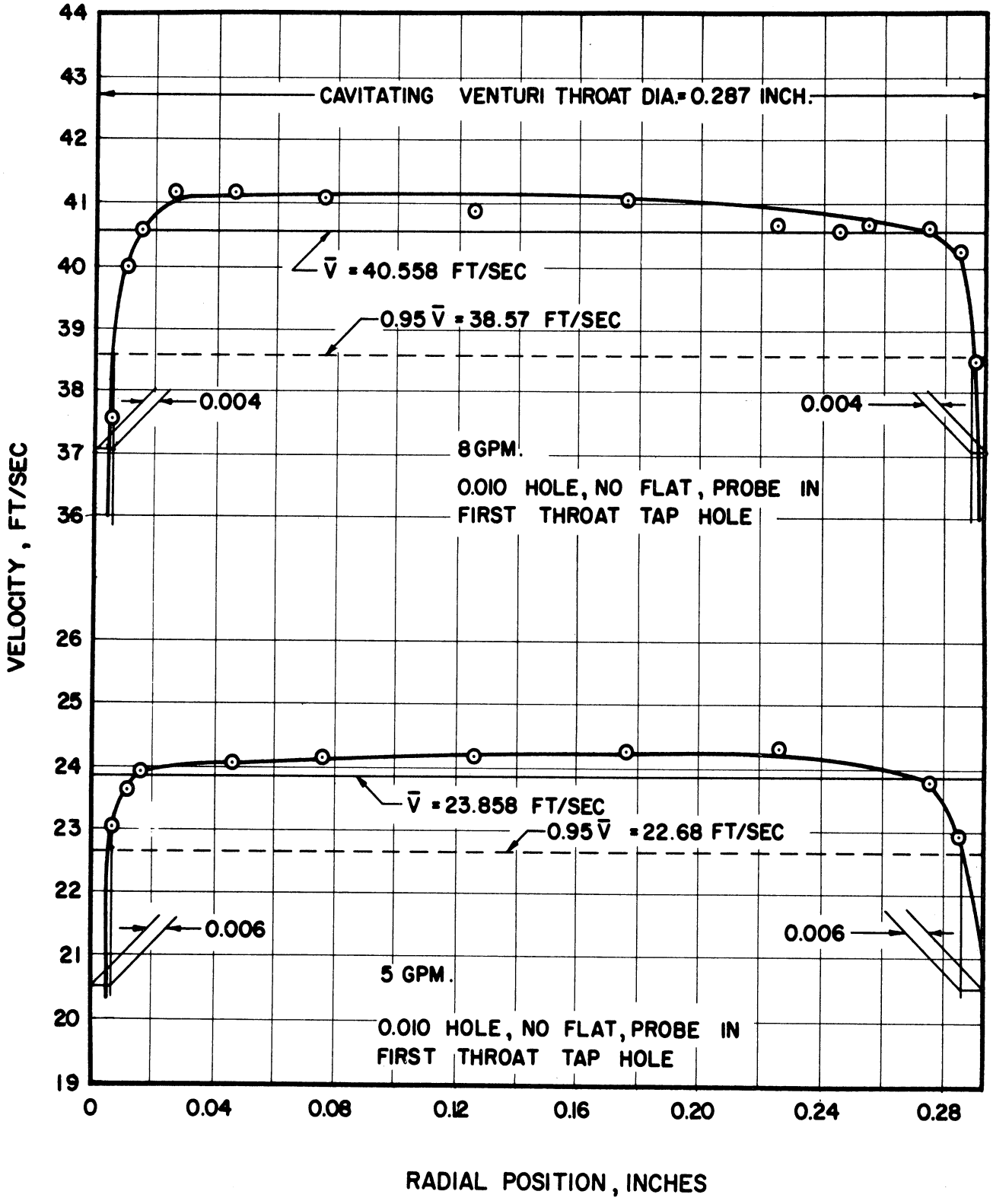

Figure 16. Throat Inlet Velocity Profiles in the Radial Direction

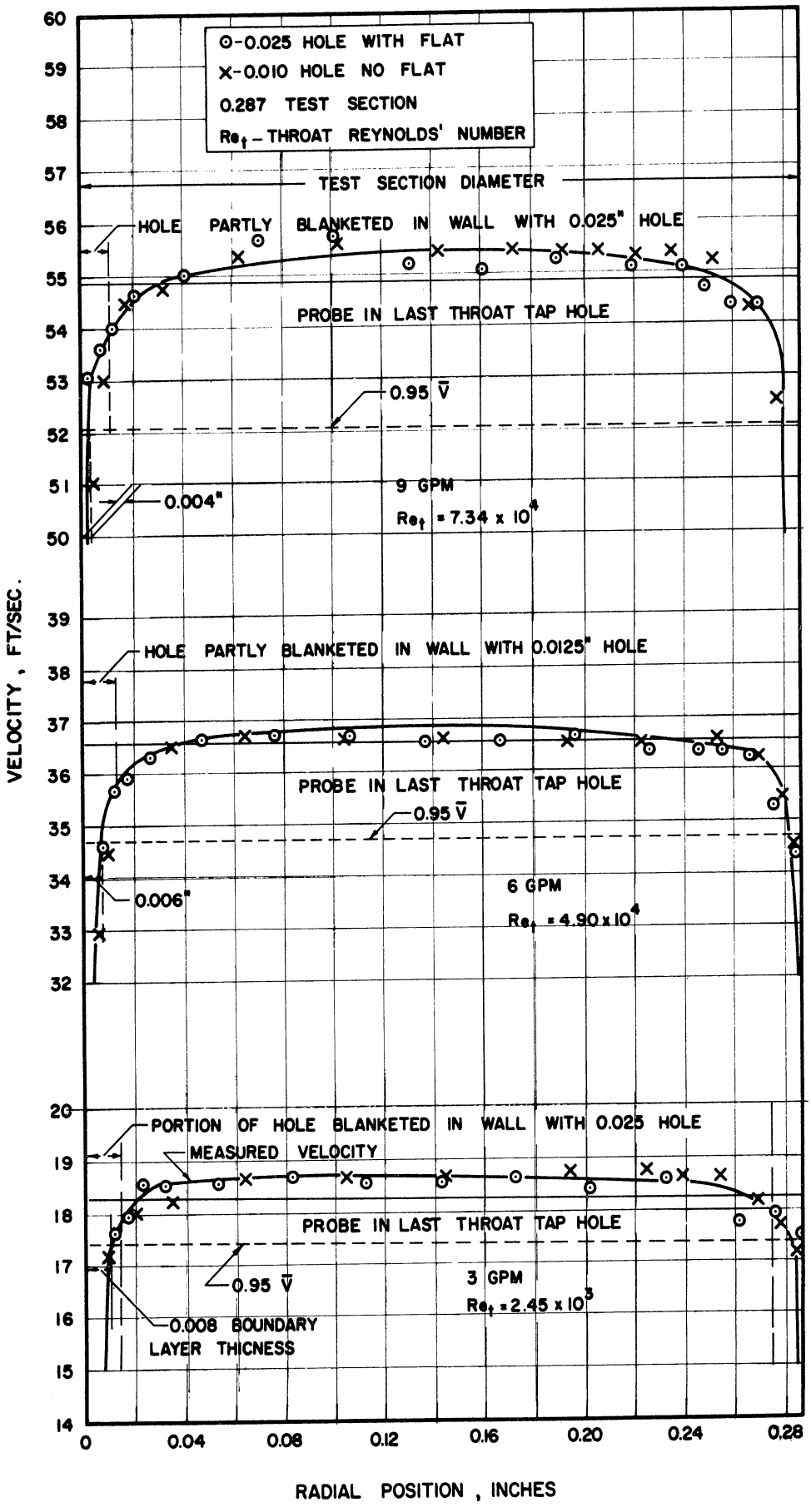

Figure 17. Throat Exit Velocity Profiles in the Radial Direction

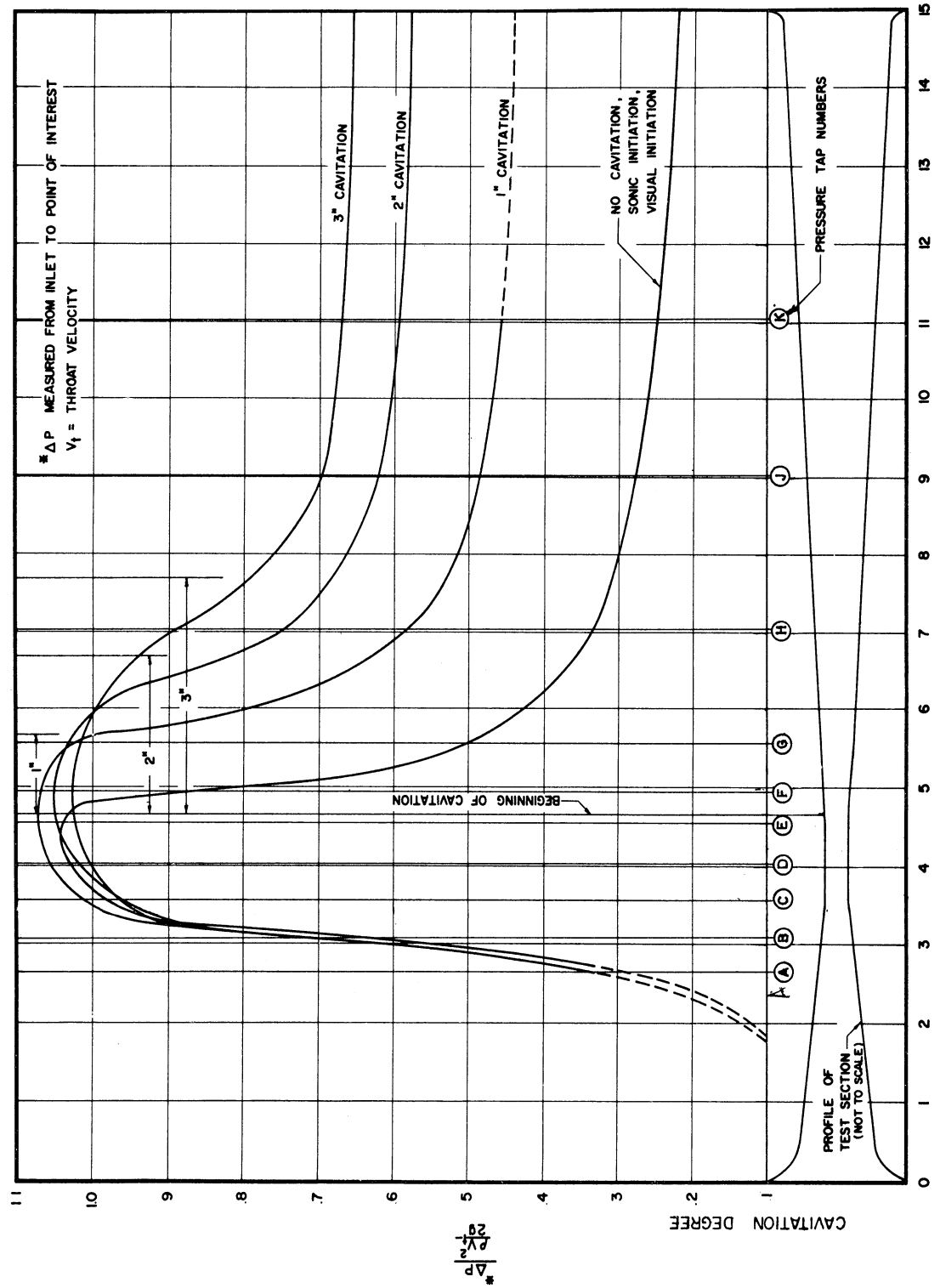

Figure 18. Axial Pressure Profiles vs. Cavitation Degree, 1/4 inch Test Section

A very flat profile exists in the throat as will be observed from Figures 16 and 17. These are the result of previous more precise velocity profile measurements in the throat region, showing a maximum boundary layer thickness of about six mils at minimum flow rate, less at higher flow rates. These were taken for the smaller test section (Figure 2) but should apply approximately to the larger. These figures are reproduced from Reference 13 for convenience. The measurements were made using a hypodermic needle similar to that described above and pictured in Figure 6, except that it included an extension beyond the hole so that it reached entirely across the section at all times into a blind hole in the opposite wall. Thus end effects are eliminated.

No evidence of separation or back-flow for the non-cavitating condition was observed (see Figures 10 - 15). This is consistent with the fact that the diffuser efficiency is of the order of 80 percent. One might expect backflow in the vicinity of the downstream termination of the cavitation region because of the severe axial pressure gradient in this vicinity (see Figure 18 for example, reproduced from Reference 13). However, the Pitot tube measurements have not indicated this. Due to their lack of precision and the uncertainty of their meaning in regions where the fluid is a mixture of liquid and vapor, it cannot be stated that such flow does not exist, and in fact it was noted to a slight degree in the high-speed motion pictures which will be discussed later.

2.2.3.2 Void Fraction and Jet Diameter from Impact Pressure Measurements

It is possible to infer the void fraction (ratio of vapor to total volume) at a given cross-section from the impact pressure measurements in two ways. These can then be compared to the void fraction as measured by gamma-ray absorption techniques and various significant conclusions drawn. The gamma-ray measurements will be described in a later section. The void fraction calculations and their results, from the impact pressure measurements, will be described here.

i) Liquid Jet Model (Method A)

If a completely liquid jet is assumed, symmetrically disposed about the center line, and surrounded by a region of complete vapor, it is possible to calculate the jet diameter based upon the known flow rate (measured by an upstream, non-cavitating flow meter) and the measured velocity in the central portion of the tube assuming an effective average velocity. This has been done (details of the calculation are shown in the Appendix), and the resulting jet diameters as a function of cavitation condition and axial position are shown in Figure 19. This simplified model is not entirely believable because of

a) High-speed motion pictures of the cavitating region showing that the portions around the central jet are actually filled with more or less spherical bubbles, presumably of vapor, in liquid. These pictures will be described in greater detail later in the report.

b) The fact that the impact pressure measurements do not fall off sharply at the outer edge of the presumed jet.

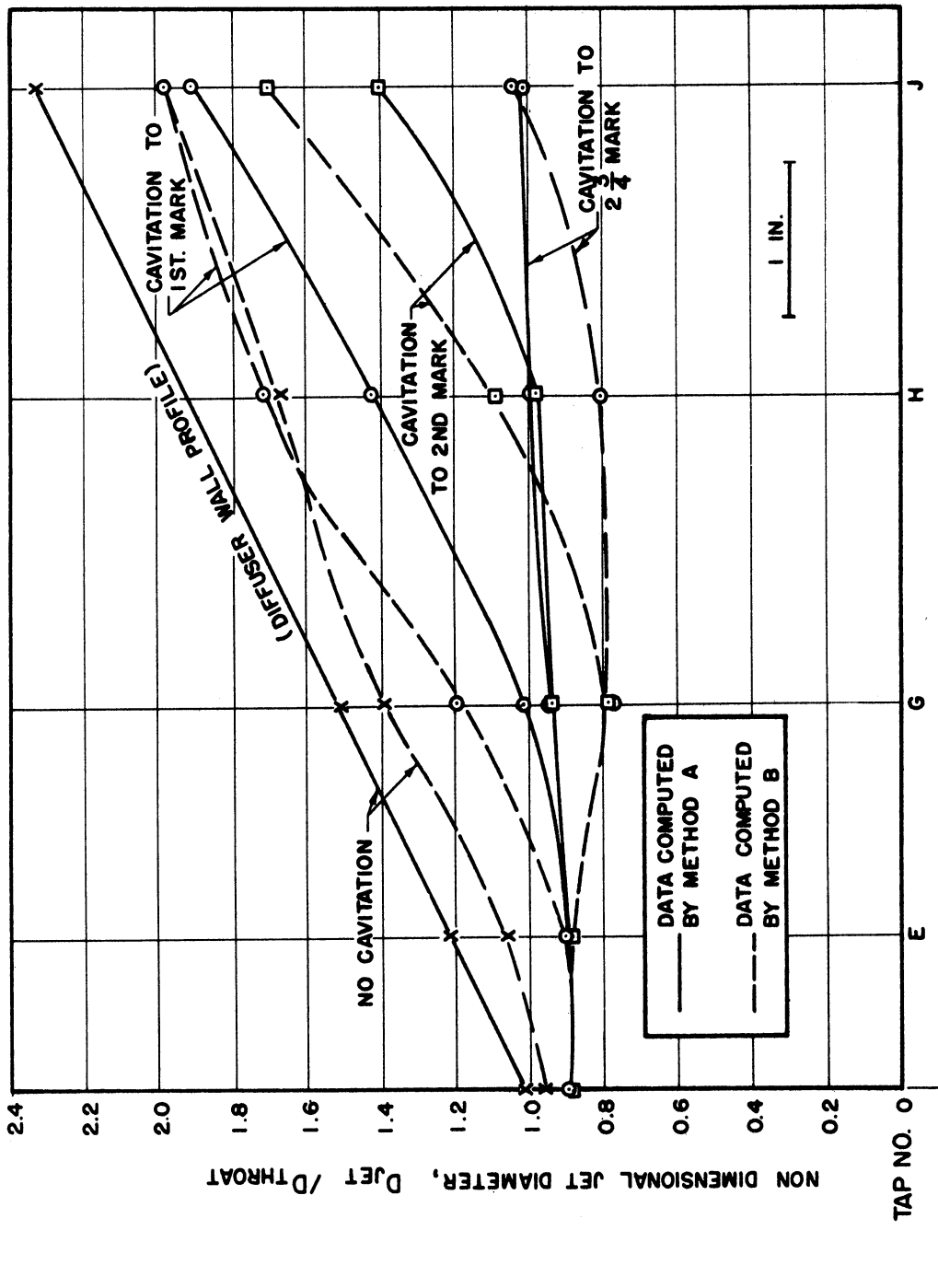

Figure 19. Comparison of Method A and B Results (Pitot-Tube Data), 1/2 inch Test Section

However, it does have the following argument in its favor, which appears to make its results more believable than that of Method B discussed later.

The velocity profile near the centerline is very flat (Figures 10 - 15), giving the appearance of the hypothesized jet. The magnitude of this velocity is only slightly less than throat velocity almost up to the apparent end of cavitation. It seems unlikely that the actual velocity could be less than that computed from the Pitot tube measurements, since all known possible errors operate in the other direction. Also it could not conceivably be substantially greater than throat velocity since no sufficient falling axial pressure gradient exists in this region. Hence the true value must be close to that measured. If this is the case, simple continuity considerations limit the jet diameter to that computed.

ii) Integrated Impact Velocity Variable Density Approach* (Method B)

If it is assumed that the fluid in any small region is composed of a homogeneous mixture of vapor and liquid (i.e.: vapor and liquid phases moving at the same axial velocity), and if the theoretical relations for the conversion from impact pressure to velocity are written, considering the reduced density in some regions, it is possible to derive a relation giving the void fraction by using the comparison between known flow rates and those integrated across the test section from the impact velocity curves. (The details of the derivation are presented in the Appendix.) Calculating back from the void fractions so derived the presumed jet dia-

* This approach and the correction involving condensate shocks were suggested by Mr. William Beckman and used by him in calculations of Reference 14.

meter can be computed and compared with that from the liquid jet model previously descrived. This is done in Figure 19. It is noted that the results are quite similar.

iii) Condensation Shock Effect

It was visually observed that a condensation shock wave or hydraulic jump formed around the Pitot tube when it was inserted into the cavitating region (Figure 7), somewhat similar to that observed in the region of collapse of the cavitation. It appears then that the static pressure in the vicinity of the probe may be considerably higher that that existing at such a location in the absence of the probe.[14] Assuming conservation of momentum across such a shock front, the velocity behind the front can be inferred if the local static pressures are known (see Appendix). To obtain improved information it is necessary to use a Pitot tube with a static as well as total pressure tap. This has not been accomplished as yet because of the restricted space. However, it is hoped that such measurements may be made eventually. In general, it is felt that Method A is more soundly based for reasons which were explained in its description. Method B relies on an assumption of no "slippage" between vapor and liquid phases, since a direct relation between volume flow rate and void fraction is assumed. It is known from numerous studies on boiling heat transfer as well as the high-speed movies discussed in this report that such an assumption is not correct.

One of the runs (Figure 20) used water heated to about 150°F while all others used ambient temperature water. For an apparent degree of cavitation, (i.e., cavitation apparently terminating

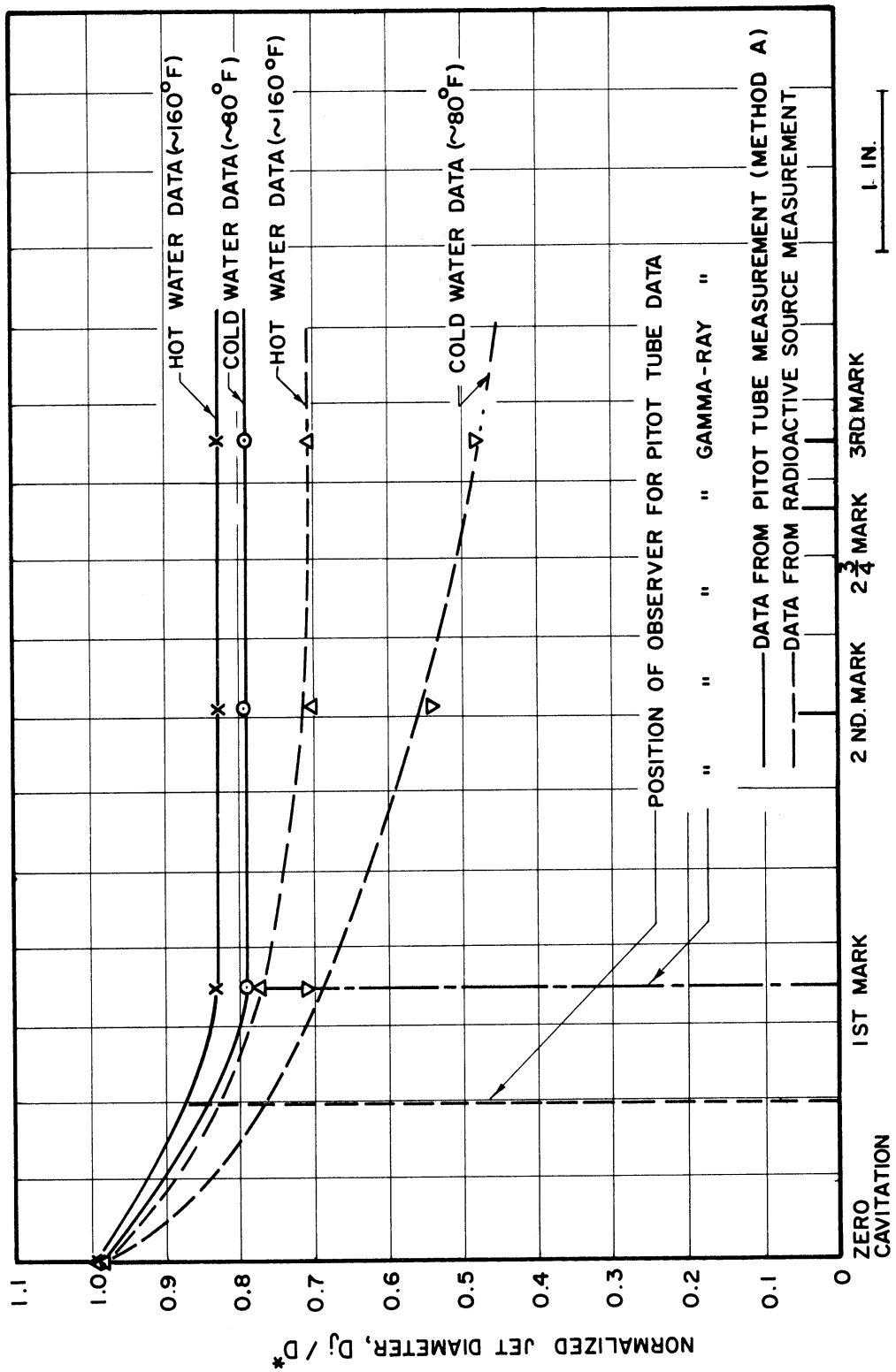

Figure 20. Comparison of Jet Diameters for Hot Water and Cold Water Runs*

* D = 0.603 For Pitot Tube Measurements
D = 0.687 For Radioactive Measurements

at a given axial location) the jet diameter obtained with hot water at a given location was less than with cold water (or the void fraction more). In other words, less fluid was evaporated, so that the mixture in the cavity contained less vapor by volume. This result agrees with that obtained by the gamma-ray measurements discussed later (and also shown on the figure). All these results are in general agreement with the predictions of Stahe and Stepanoff[15] and the observations of Salemann[16] using a centrifugal pump. They are inferred from the much greater volumetric latent heat of hot water as compared with cold water. The effect can be expressed by the ratio $[\rho_V C(\Delta T/\Delta H)]/\rho_L h_{fg}$ given previously by one of the present authors in Reference 17 or in a somewhat different form by Stahl and Stepanoff[15],

where: ρ_V = vapor density
ρ_L = liquid density
C = specific heat of liquid
$\Delta T/\Delta H$ = change of temperature per unit change in saturation head
h_{fg} = latent heat of evaporation.

2.3 Gamma-Ray Absorption Tests

2.3.1 General Criteria

It was desired to measure with reasonable precision the void fraction in the cavitating venturi as a function of axial position, cavitation condition, and other applicable fluid parameters such as temperature, velocity, aereation, etc. At the time of the planning of the experiments no information on the magnitudes to be expected was available, as no similar measurements are reported in the literature.

It was arbitrarily postulated that the detection of void fractions as low as two percent would be necessary, and the experiment was planned partially as a feasibility test to see if measurements of sufficient precision to detect the void fractions actually existing could be made. If feasibility were demonstrated, additional tests could be made in the future in which the location of the voids was more accurately measured and the effect of various of the fluid parameters more carefully examined. The preliminary tests only are herein reported. Future, more precise, tests are planned, as it has been demonstrated by these initial tests that the void fractions are considerable, and well within the precision of the equipment.

To attain a given degree of precision, it is necessary that the difference in count rates obtained between measurements with and without voids be statistically significant. Also it is necessary that the total count be obtained in a reasonably short length of time; no more than perhaps one minute, since the maintenance of steady-state flow conditions over a long period is difficult. Also the time consumed in testing over a large number of conditions and locations would become prohibitive.

Sufficiently high count rates can be always attained theoretically by using a source of a sufficient number of curies. However, in practice there is a limit because of requirements for safe handling, and the necessity of concentrating the source sufficiently to allow it to be considered as a point source of known location. The sensitivity of

count rate to void fraction can be increased if the photon energy of the source is decreased, the absorption coefficient increasing rapidly in such cases. Such a sensitivity increase decreases the required total count (or count rate, if a time limit is imposed) to attain the desired degree of precision. However, decrease of photon energy, and consequent increase of absorption coefficient, means a smaller count rate for a given number of curies in the source, so that the practical limitation on source size may be encountered.

2.3.2 Apparatus

In the present case where cavitating water venturis of either 1/2 or 1/4 inch nominal throat diameter were to be used, it was necessary that the absorption coefficient be very high, if sufficient precision was to be obtained. If mercury were tested in the same venturis, the absorption coefficients for photons of a given energy would be increased at least in proportion to the fluid density, so that the problem is not nearly so difficult.

In the case of water, calculations indicated that none of the common gamma-ray emitters were of sufficiently low energy. Photon energies in the range of conventional X-rays were required. However, an X-ray machine was not feasible because of space limitations as well as economic considerations.

A solution was effected by the use of a promethium-tungstate, $(Pm_2^{147}WO_4)_3$, source-target mixture. The original studies on the use of this material are described in Reference 18, and the details of its

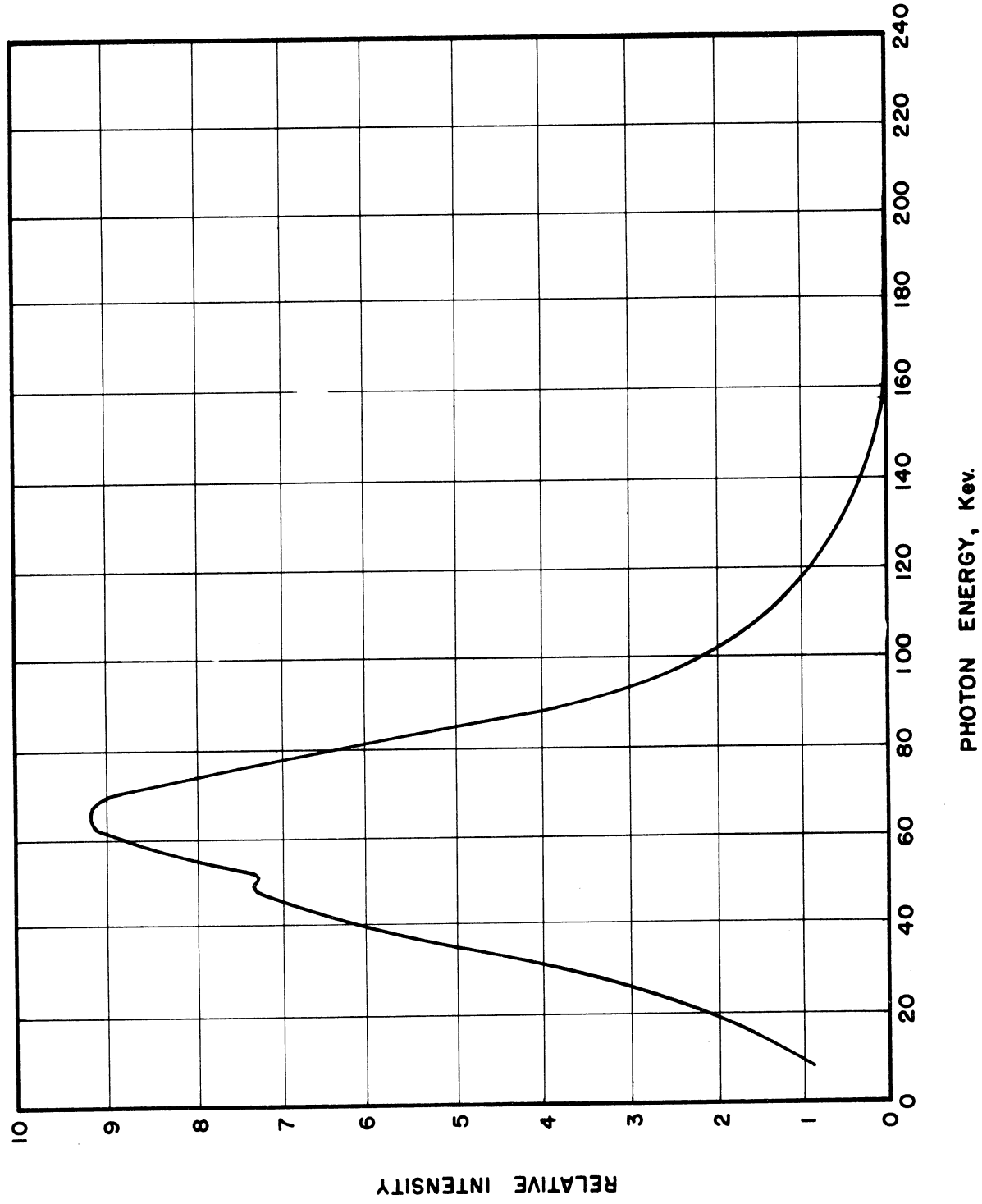

Figure 21. Energy Spectrum of $(WO_2)_3Pm_2^{147}$ Source

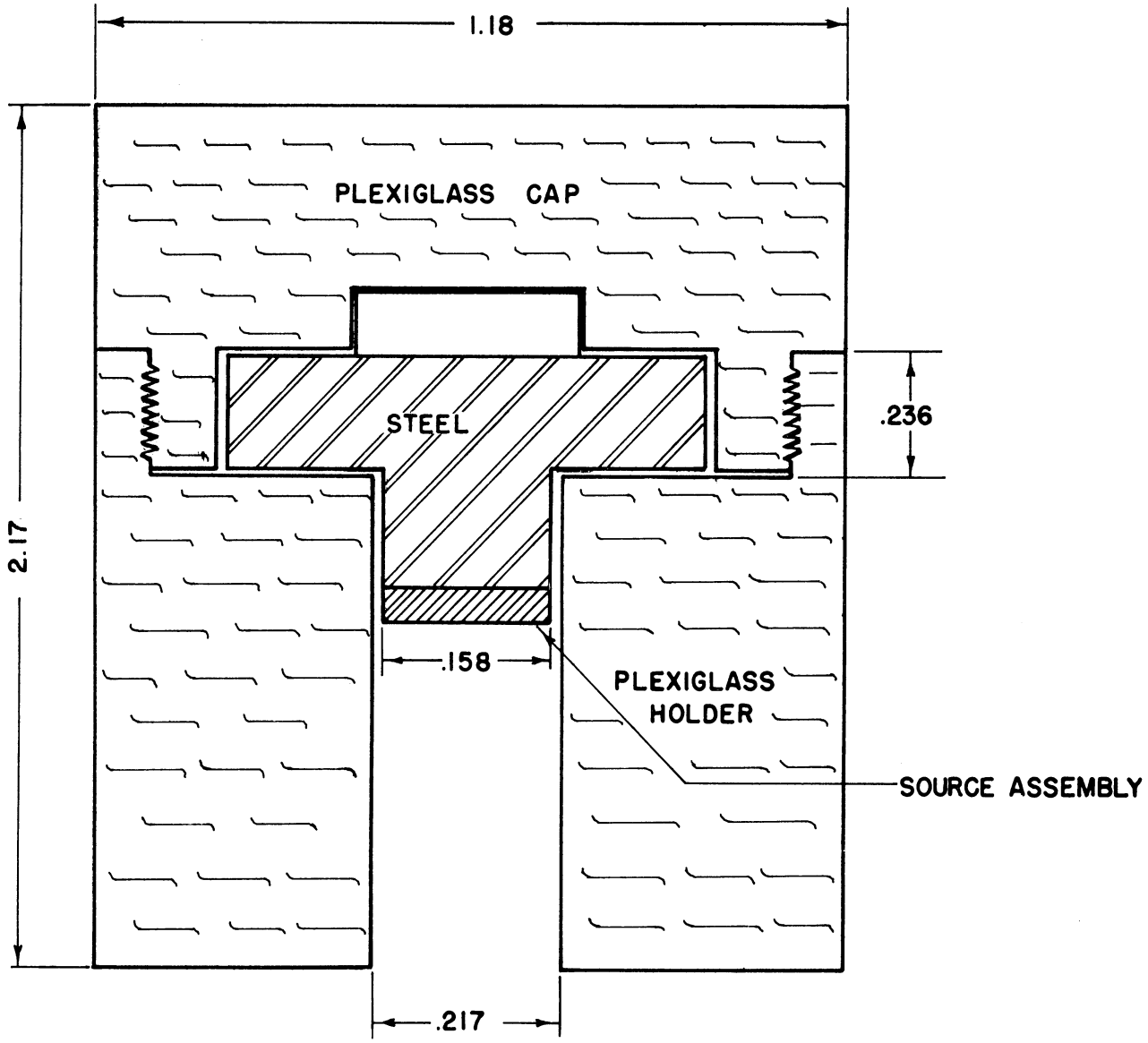

Figure 22. Promethium-Tungstate Source and Holder (Schematic)

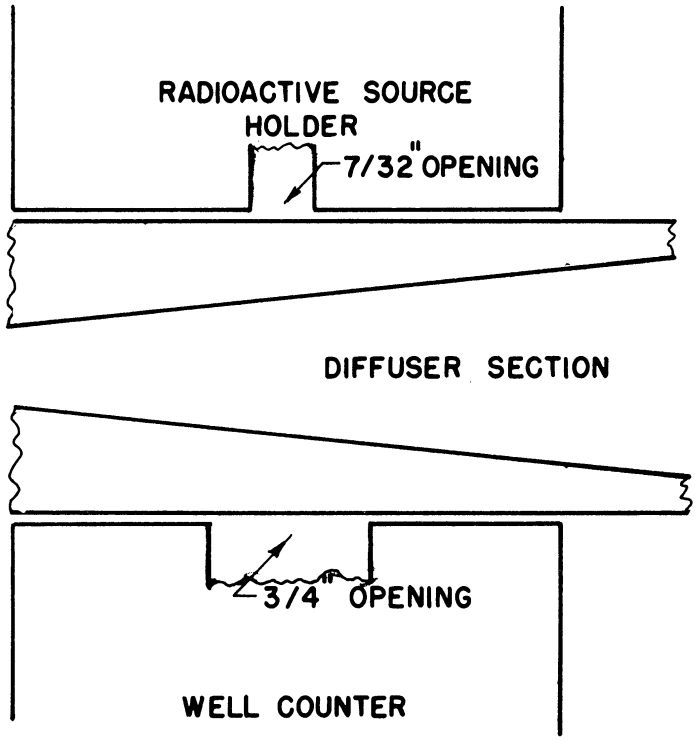

Figure 23. Schematic Diagram for Radioactive Source Measurement Arrangement

use in the present application in Reference 19, the significant points of which will be summarized here. The mechanism for the production of low energy photons is as follows: Pm^{147} is a pure beta emitter; the betas (223 Kev) impinge on the tungsten, causing the emission of K-capture photons. In addition bremsstrahlumg X-rays are emitted from the various materials of mixture and container so that a fairly continuous spectrum is provided as from an X-ray tube. The characteristic energy vs. intensity plot for the mixture is given in Figure 21. It is noted that the relative intensity peaks quite sharply at 66 Kev, but that there is significant intensity between about 10 and 140 Kev.

The half-life of the promethium (which is of course the significant time constant) is 2.6 years, so that deterioration is not inconveniently rapid. The source at the time of use had an intensity of about 0.5 curies.

The source (Figure 22) was encapsulated in a modified standard Oak Ridge capsule. This was placed in a plexiglass holder which was used to eliminate the possiblity of accidental contact with the source during handling.

A schematic representation of the experimental set-up is shown in Figure 23. The source was placed above the large (1/2 inch throat) venturi, as close to it as possible, and a shielded-tube, RCL scintillation-type well-counter below. In these preliminary experiments, no collimation was used, so that the data does not give radial location of voids, but rather a gross void measurement for a given cross-section.

2.3.3 Experimental Results

2.3.3.1 Calibration Experiments

Calibration experiments were made to be sure that the results would be meaningful. A constant diameter, cylindrical model of the test section with similar wall thickness and a typical, uniform bore, and of the same material (plexiglass) was fabricated. By volume measurement, it was possible to determine accurately the portion of the cross-section filled with water when the model was mounted horizontally. Count rate measurements were made for various water depths. It was found that the relation between count rate and portion of path filled with water was essentially linear. These results, for both collimated and non-collimated set-ups, are shown in Figure 24. Although the actual attenuation of the gamma-ray beam is, no doubt, exponential, the degree of attenuation in the short passage through the absorber is so small that it can be considered linear. If this is the case, the portion of the path through the test section which is through liquid (rather than gas (gas absorption is effectively zero) can be determined if two extreme conditions

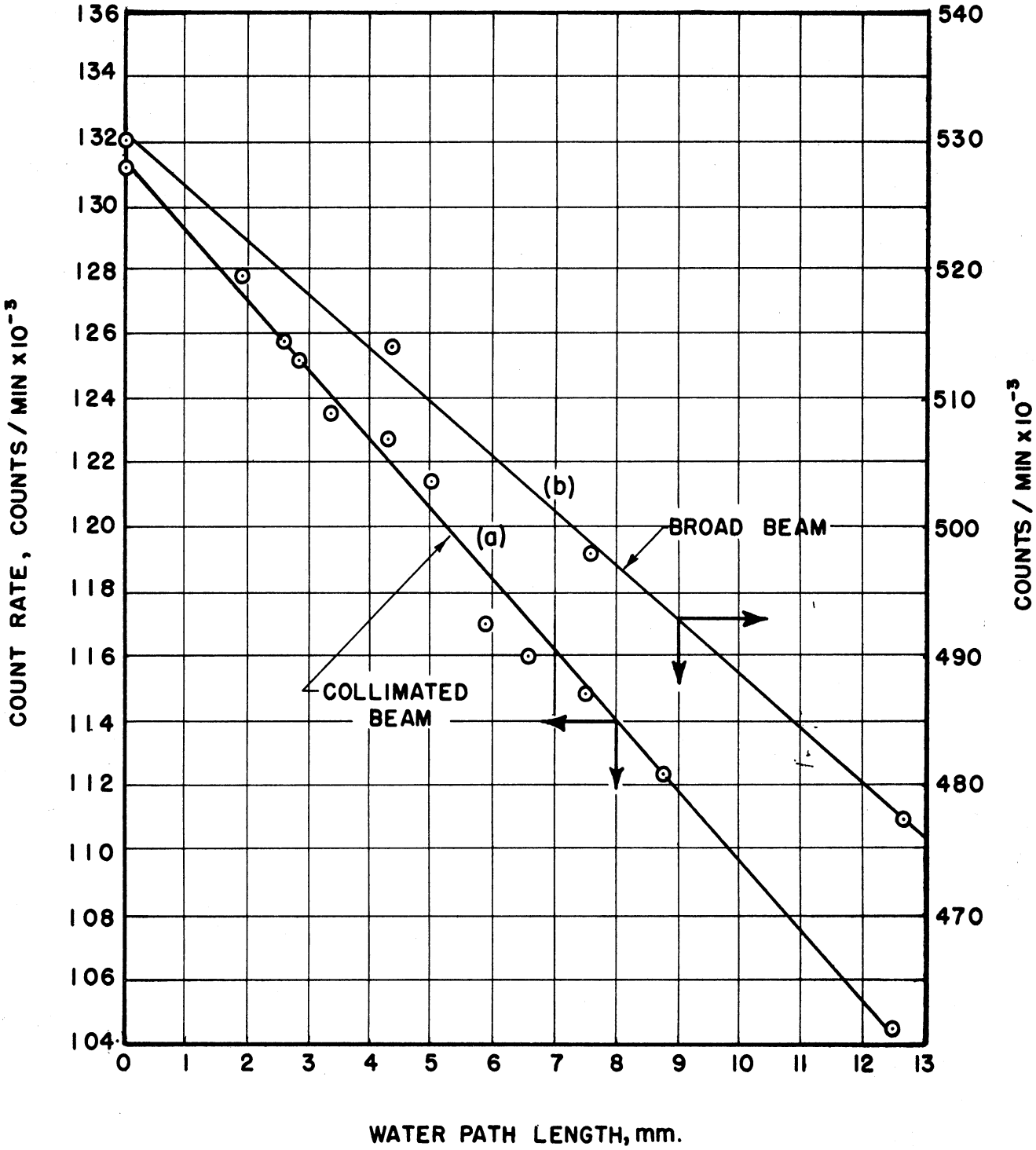

Figure 24. Source Calibration for Void Fraction Measurements (Water Path Length in Model Test Section vs. Count Rate)

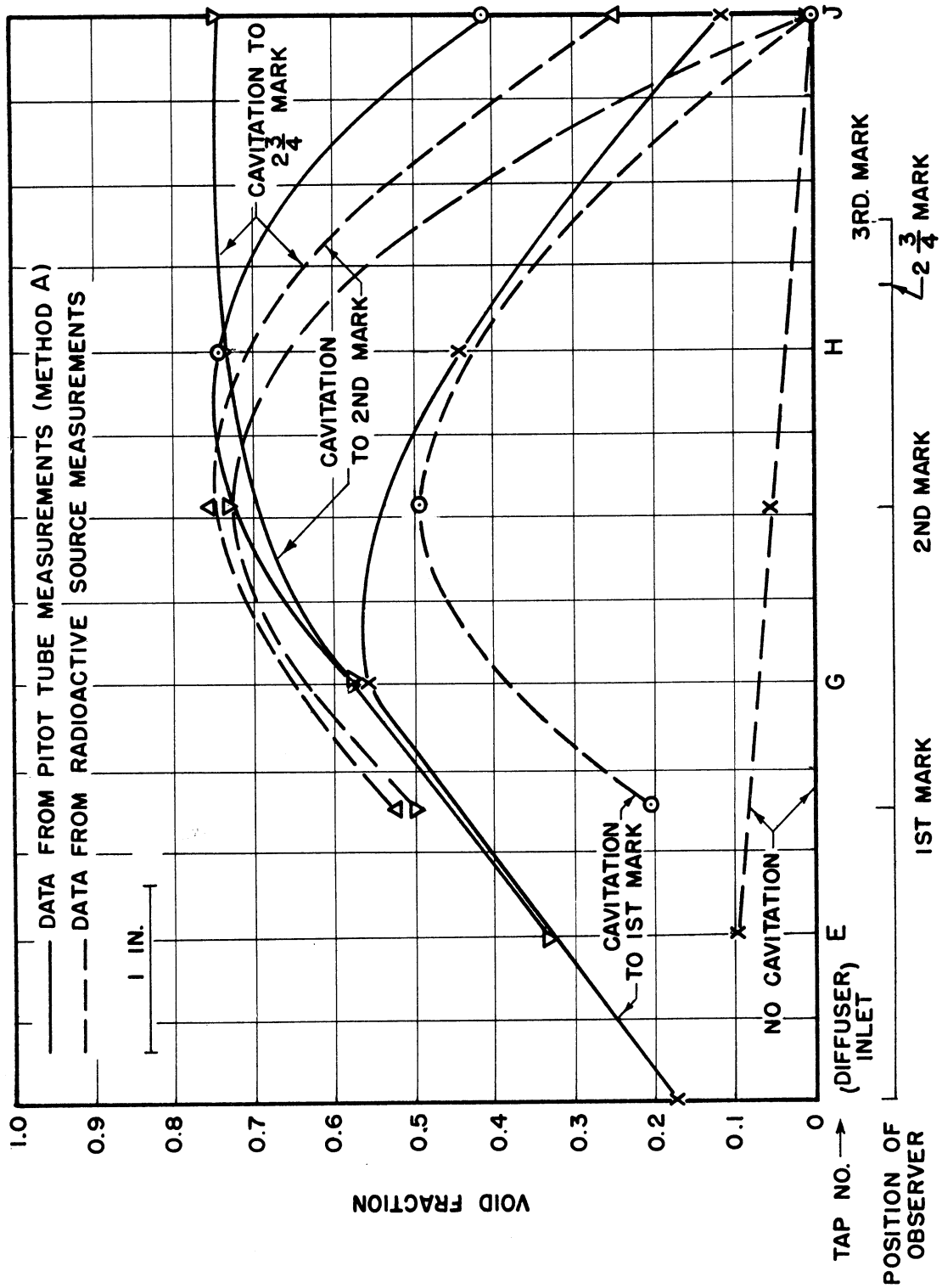

Figure 25. Void Fraction as a Function of Position of Observer and Cavitation Condition

are known. As used in the actual experiment, these conditions correspond to all liquid and zero liquid, i.e., empty. Then the following relation was used:

$$\frac{\text{Fluid Path Actual}}{\text{Fluid Path (Full)}} = \frac{N_{empty} - N_{actual}}{N_{empty} \quad N_{full}}$$

where N is the count rate per unit time, and the subscripts are self-explanatory.

2.3.3.2 Cavitation System Experiments

If it could be considered that the cavitating flow pattern is a central liquid jet surrounded by vapor, as described previously, and that the gamma-beam is sufficiently narrow and well-centered to penetrate only the liquid portion, then this ratio can be used to compute the jet diameter (see Appendix). This has in fact been done and the results are shown in Figure 8 previously described, where they are compared with the results taken from the Pitot-tube runs. The comparion has also been previously discussed. Figure 25 shows the void fractions directly from these and the Pitot tube measurements. The void fractions measured are considerably greater than the original anticipation, being actually up to 75 percent. The experiment was planned to yield a precision of approximately ± 2 percent, so the experimental error is believed small compared to the measured magnitudes. As mentioned in the discussion of the Pitot-tube measurements, one of the runs used heated water. The results are shown in Figure 20 and have been discussed previously.

2.4 Significance of Void Fraction and Jet Diameter Measurements by Pitot-Tube and Gamma-Ray Absorption

The jet diameters inferred from Pitot-tube and gamma-ray measurements at different axial locations as a function of cavitation condition have been compared in Figure 8; the void fractions in Figure 25. Since jet diameter and void fraction are uniquely related, the following discussion applies to either.

While there is not perfect agreement between the measurements, particularly in regions far from the throat, it is noted that the agreement near the throat is quite close. Substantial reasons for a lack of agreement, beyond the inherent inaccuracies of the methods, may be advanced.

Basically, the gamma-absorption technique and the Pitot-tube technique do not measure the same thing. The gamma-ray instrument measures directly the ratio of vapor to total volume but is insensitive to velocity. The Pitot-tube is sensitive to the product "(velocity squared)x (density)". In regions where the fluid may be stagnant, it cannot distinguish between vapor and liquid.

On the basis of the above reasoning, it might be expected that the Pitot-tube measurements would indicate the persistance of the apparent small velocity jet further downstream than would be indicated by the void fraction measurements. Suppose that near the throat there is actually a jet of liquid surrounded by a region largely vaporous. Further downstream, the vapor region will be terminated as the pressure starts

to rise and the vapor to condense. However, the fluid near the wall is presumably relatively stagnant, and there may even be back flow because of the sharp axial pressure gradient in this vicinity. Proceeding still further downstream, the influence of the central, high-velocity, liquid jet makes itself felt in the surrounding liquid by the action of turbulent shear, so that the fluid, now almost all liquid, assumes a more normally distributed velocity profile typical of the Reynolds number and rate of divergence of the diffuser. Thus, the jet, as inferred from Pitot tube measurements, would persist after the collapse of the vapor, whereas that inferred from gamma-ray absorption would terminate with the vapor region.

Further precise delineation of the flow pattern in the cavitating region will require knowledge of the make-up of the vaporous region. It is necessary to know either the relative velocity between liquid and vapor phase, or the local quality. It may be possible to obtain some information on the relative velocity by refined photographic techniques. Preliminary results of this sort have been obtained and will be discussed in a later section. However, gamma-ray void fraction measurements, wherein close collimation is used and the location of the photon beam is accurately known, would allow the calculation of local quality if axial symmetry were assumed (which seems reasonable). Future tests of this sort are planned. Direct quality measurements in a region of presumably low quality, using standard thermodynamic techniques do not seem possible, although theoretical feasibility investigations along this line might be fruitful.

Another possible approach would involve measuring sound velocity and acoustic impedence in the region of interest and attempting to correlate with the void fraction. Work of this type is reported in the literature[20].

2.5 High-Speed Motion Pictures

2.5.1 General Objectives

To gain further insight into the nature of the flow in cavitating venturis than could be obtained through ordinary visual observation, or through the Pitot-tube or gamma-ray techniques previously described, pictures of sufficient speed to "stop" the flow would be most desirable. In this way it might be possible to gain some information on the contents of the cavitating region, on the velocities of liquid and vapor phases in this region, absolute and relative to each other, and on the general flow pattern existing.

The test section available was circular rather than two-dimensional, so that the exact determination of conditions in a given plane is difficult. However, as previously mentioned, the general objectives of this project are the comparison of cavitating effects in a flowing system between different fluids, including high-temperature liquid metals and perhaps cryogenic fluids. It is desired to develop a suitable type of test section and use it throughout; hence, considerations of mechanical simplicity require a simple circular section. Nevertheless, certain preliminary semi-quantitative results have been obtained and these will be described in later paragraphs.

2.5.2 Apparatus

A 16mm Fastax camera was used in the high-speed motion picture study. The camera is capable of 8000 frames per second. At the 8000 framing rate, the effective film exposure time is 41.7 microseconds with the standard 16mm aperature. In this study a .040 slit was inserted in front of the standard aperature. With the .040 insert the film exposure time was reduced to 16.7 microseconds. Required duration and intensity of the light flash (film exposure) is of major importance. The general criterion is that the bubble should not move more than its own diameter during the duration of the flash. For example a 70 foot per second velocity was used in several of the tests. Then with the effective 16.7 microsecond flash duration, a bubble of 14 mil diameter would be the minimum size meeting this criterion.

A two inch coated f/2.7 lens with minimum focal length of 28 inches, was used with the high speed camera. Because of the high light intensity needed with the effective exposure time, a new type light source was used. This consisted of an FF-33 flood flashlamp, fabricated with a magnesium foil, which gives a plateau average light level of 75,000 lumens over a time interval of 1.75 seconds. An illumination of 200,000 foot-candles can be achieved in a seven inch highly polished reflector when the lamp is flashed with the base down, at a twelve inch light-to-object distance. Even with this required light the guide number is such that the lens must be fully opened. Another consideration was that a flash bulb of this type develops a relatively small amount of heat and therefore there would not be damage to the plexiglass test section. This problem would be encountered with normal flood lamp illumination of sufficient intensity.

2.5.3 Results Obtained

2.5.3.1 General Flow Pattern

In the preliminary tests which are reported here, it was not possible to get a clear picture of the entire cavitating region. The lighting was such that the collapse region was not clearly photographed. It is hoped in future tests that this difficulty can be overcome. However, good pictures were obtained of the regions where visible cavitation first appeared and where it becomes well developed. Figure 26 shows typical frames taken at about 8000 frames per second. The vaporous region appears to be filled with discreet, fairly large bubbles moving at high velocity rather than a more or less homogeneous vapor-liquid mixture as might have been surmised. Tracing of bubbles from frame to frame has showed that they are moving downstream with a velocity of about 7/8 that of the central jet liquid velocity. However, near the point of termination of the vapor region, there appears to be some back-flow, as might be intuitively expected on the basis of the steep axial pressure gradient in this region.

Considering reported observation of two-phase flow in the boiling heat transfer literature, it is probable that there is some slippage between the vapor and liquid phases. A numerical value cannot be inferred, however, since no measurements of local liquid velocity in the vaporous region are available (see previous discussion on the Pitot-tube measurements).

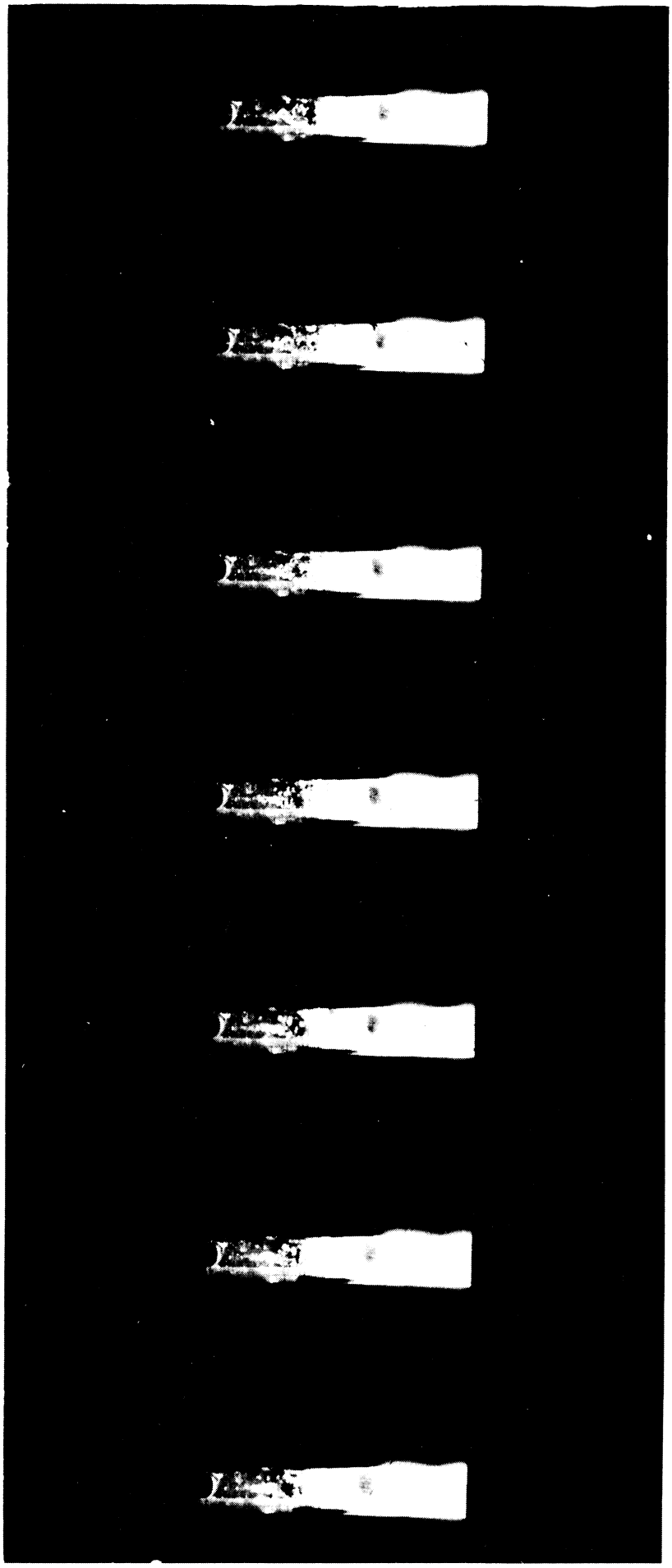

Figure 26. High Speed Motion Pictures of Cavitation Phenomenon

It has been reported by Knapp[21] from a high-speed motion picture study of a somewhat similar vapor region attached to an ogive test section in the CIT water tunnel, that periodic oscillations of the length of the cavity occurred. A somewhat similar observation was made earlier by Nowotny[1]. In the present case, the flow in the vicinity of the cavitating region is certainly not steady-state when examined with a high-speed motion picture camera although no fluctuations are visible to the unaided eye. The point of initiation and termination appear to vary to some extent so that the length of the cavitating region also fluctuates. So far it has not been possible to determine the period of such fluctuation, although futhure tests may assist in this matter.

As noted from Figure 26 the bubbles appear to be roughly spherical, varying in diameter from about 1/32 inches to 3/8 inches. The mean maximum-growth diameter for all observed bubbles is about 1/8 inches. This information comes from a detailed inspection of the motion picture frames, where 160 bubbles were traced over several frames. The maximum-growth-diameter distribution is shown in Figure 27, for some 40 random bubbles.

Figure 28 shows the bubble velocity distribution in a similar manner.

Figure 29 shows rate of bubble growth distribution. This has been calculated from observed bubble dimensions in various frames and the known time interval between frames. The average growth

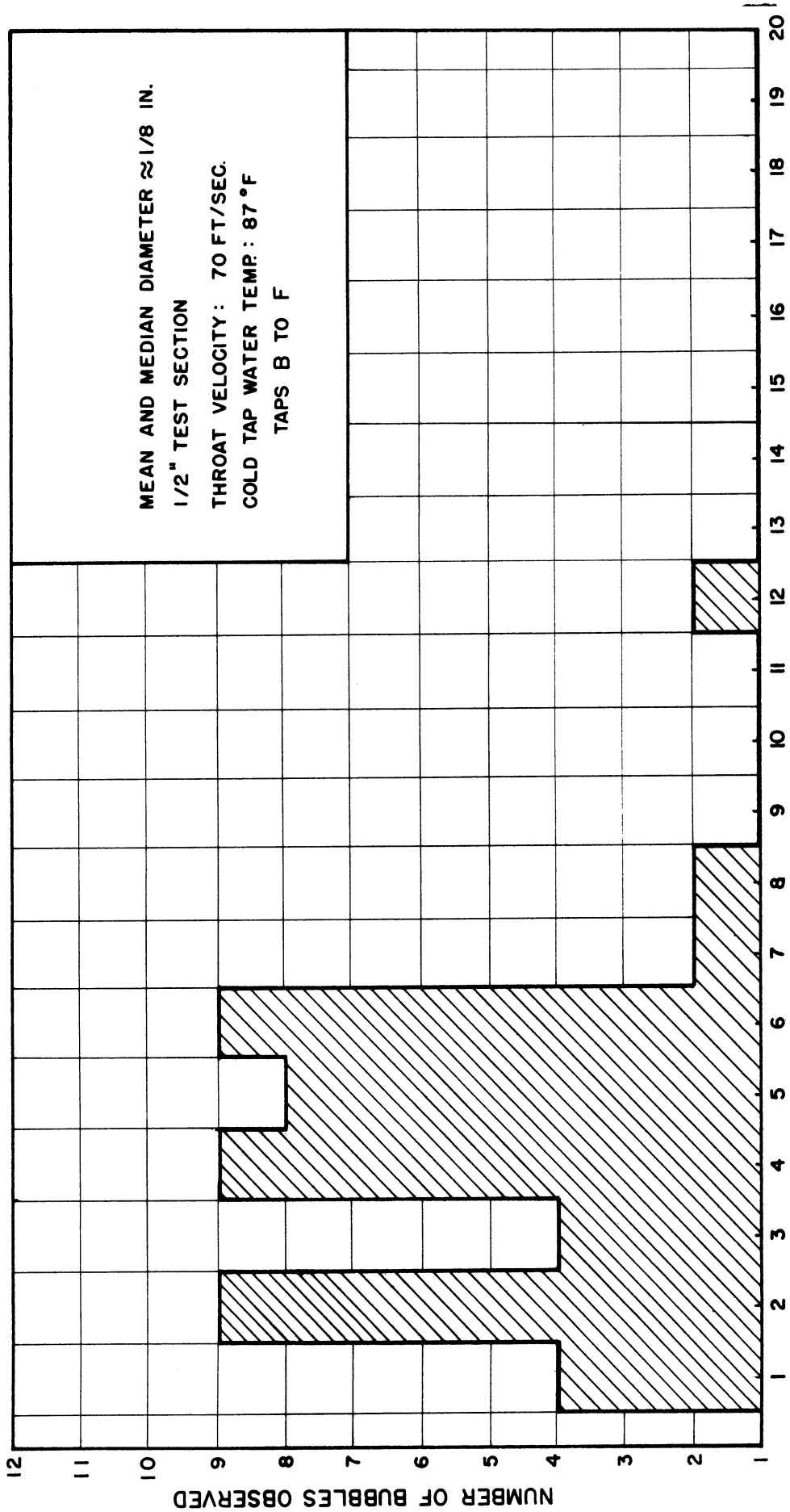

Figure 27. Bubble-Maximum-Growth Diameter Distribution

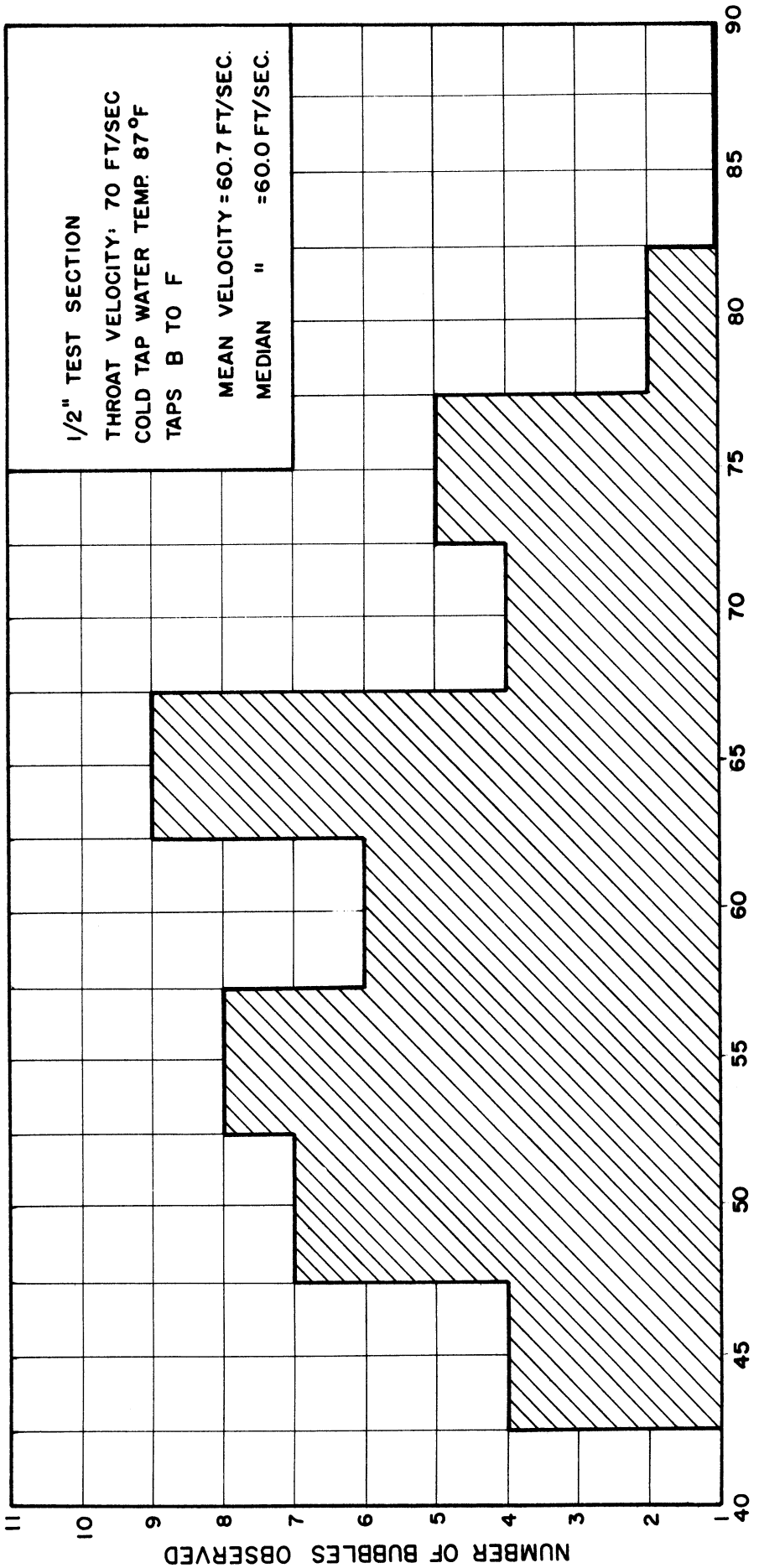

Figure 28. Bubble Velocity Distribution

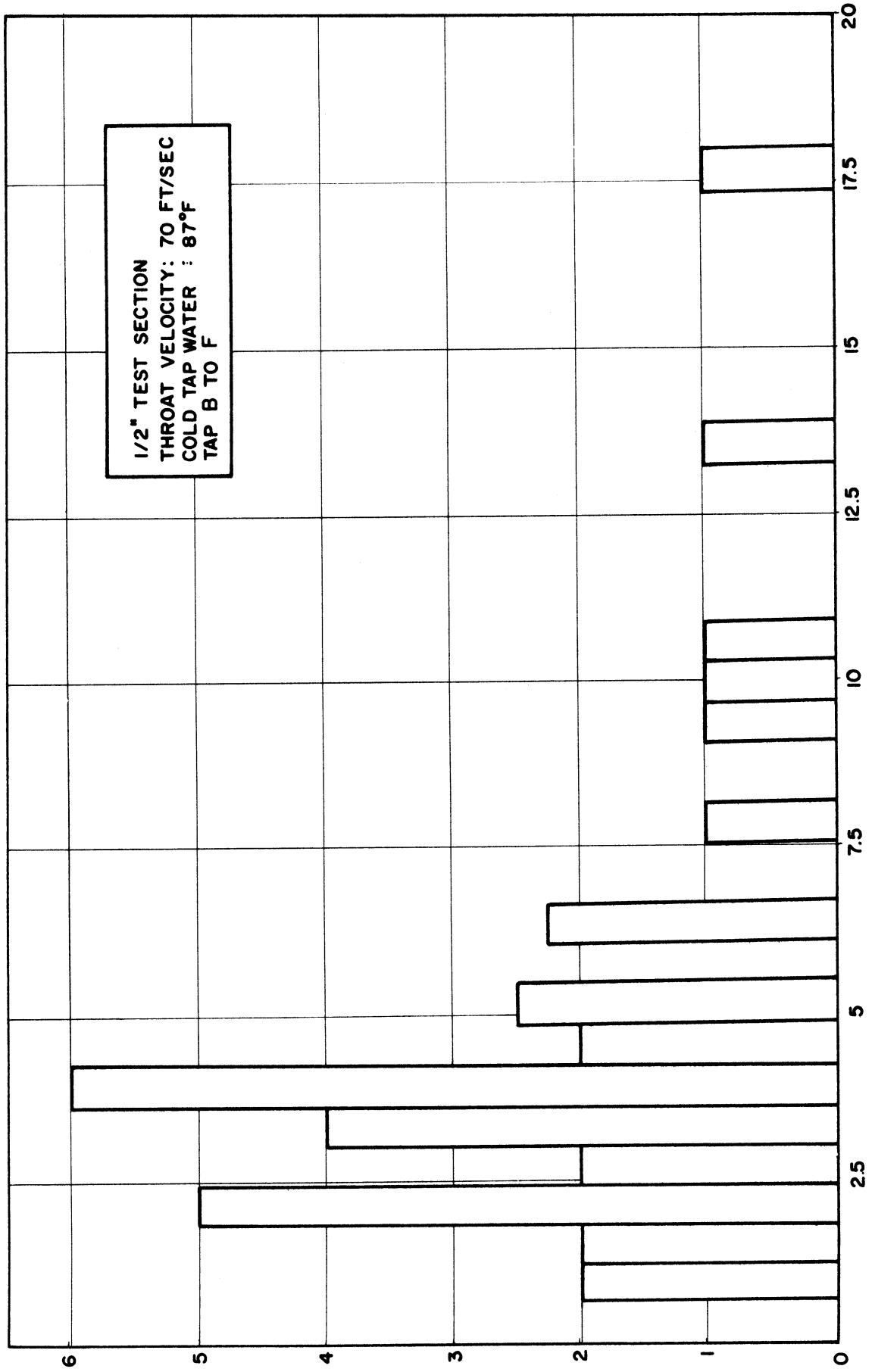

Figure 29. Bubble-Growth-Rate Distribution

velocity under the conditions observed (70 feet per second throat velocity) is about eight feet per second. However, the maximum observed is about 40 feet per second. In some cases, as Figure 26, it was also possible to follow the collapse of a bubble. In this particular case, the collapse velocity between the observed diameters of 0.1875 and 0.0188 inches was about 19 feet per second.

Figure 30 sketches and describes the general flow pattern observed from the motion pictures. As previously mentioned the initiation region was shown clearly but the collapse region was over-exposed. It is hoped that this can be corrected in the next series of tests.

As shown in Figure 30, some of the bubbles appear to initiate from pressure tap C (Figure 3), whereas the main cavitation appears near the next tap, D. In between, there sometimes appear arrowhead or "T" formations of bubbles, at the head of which there is usually one or more distinct bubbles.

3.0 Conclusions

Quantitative and semi-quantitative measurements and observations have been presented to describe the nature of flow in a cavitating venturi. Detailed pressure and acoustic measurements will be presented in future reports.

In general, it is verified that the flow pattern is somewhat similar to that of a free jet issuing from the throat surrounded by a region primarily vaporous. The jet undergoes a

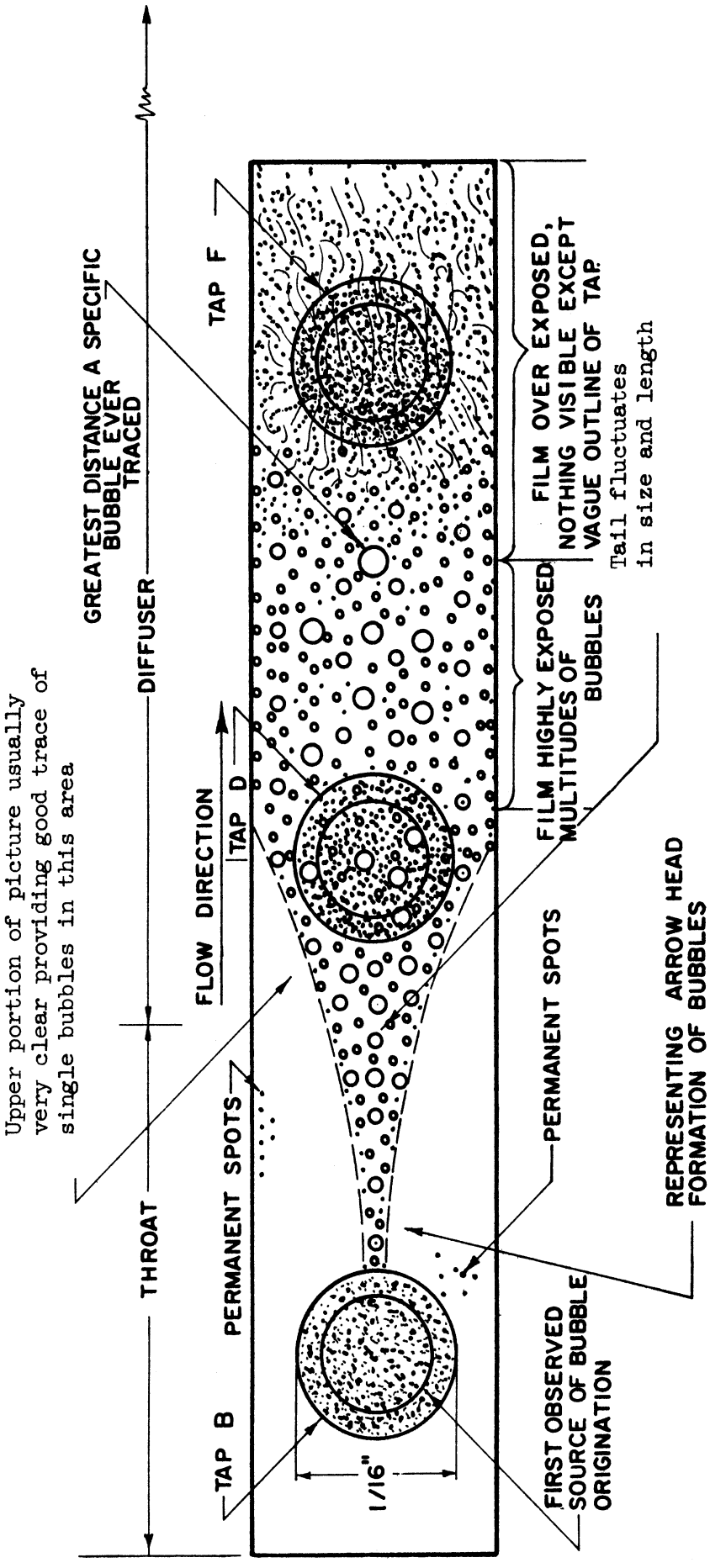

Figure 30. Sketch of Cavitating Region in Motion Pictures

phenomenon similar to a hydraulic jump, or a normal condensation shock in which the static pressure is raised considerably. In this region the vaporous region terminates and the flow becomes a single-phase liquid flow.

BIBLIOGRAPHY

1. Nowotny, H., "Werkstoffzerstorung durch Kavitation," VDI-Verlag GMBH, Berlin, 1942 (Published in U.S. by Edwards Brothers, Inc., Ann Arbor, Michigan, 1946).

2. Hunsaker, J. C., "Cavitation Research - A Progress Report on Work at MIT." Mech. Engr., April, 1935.

3. Wright R. S. and Olicker, S. D., "Cavitating Venturi for Flow Control," Chemical Engineering, November, 1956.

4. Randall, L. N., "Rocket Applications of the Cavitating Venturi," American Rocket Society Journal, 22, No. 2, Jan.-Feb., 1952.

5. Eisenberg, P., "A Brief Survey of Progress on the Mechanics of Cavitation," DTMB Report No. 842, June, 1953.

6. Eisenberg, P. and Fitzpatrick, H. M., "Cavitation Inception and Measurement of Air Content," Proc. American Towing Tank Conference, University of Californiz, August 31 - September 2, 1959.

7. Eisenberg, P., "On the Mechanism and Prevention of Cavitation," DTMB Report No. 712, July, 1950.

8. Kermeen, R. W., McGraw, J. T., and Parkin, B. R., "Mechanism of Cavitation Inception and the Related Scale-Effects Problem," Trans. ASME, May, 1955.

9. Strasberg, M., "The Influence of Air-Filled Nuclei on Cavitation Inception," DTMB Report No. 1078, May, 1957.

10. Straub, L. G. and Olson, R. M., "Cavitation Testing in Water Tunnels," University of Minnesota, St. Anthony Falls Hydraulic Laboratory, Project Report No. 42, December, 1954.

11. Straub, L. G., Ripken, J. F., and Olson, R. M., "A Study of the Influence of Gas Nuclei on Cavitation Scale Effects in Water Tunnel Tests," University of Minnesota, St. Anthony Falls Hydraulic Laboratory, Project Report No. 58, February, 1958.

12. Holl, J. W., "An Effect of Air Content on the Occurence of Cavitation, ASME Paper No. 60-HYD-8.

13. Hammitt, F. G., "Liquid-Metal Cavitation-Erosion Research Investigation, Final Report," University of Michigan Research Institute Report No. 2824-3-F.

14. Beckman, W. and E. Flanigen, "Void Fraction Measurements," Term Paper, ME-200, Mechanical Engineering Department, University of Michigan, June, 1960.

15. Stahl, H. A. and Stepanoff, A. J., "Thermodynamic Aspects of Cavitation in Centrifugal Pumps," Trans. ASME, Vol. 78, 1956, pp. 1691-1693.

16. Salemann, V., "Cavitation and NPSH Requirements of Various Liquids," Trans. ASME Series D, Journal of Basic Engineering, Vol. 81, 1959, pp. 167-173.

17. Hammitt, F. G., "Liquid-Metal Cavitation-Problems and Desired Research", ASME Paper No. 60-HYD-13.

18. Coleman, E. W., Brownell, L. E., Fox, C. J., "Studies on X-rays and Bremsstrahlung for Source-Target Mixtures," Project Report No. 2471-2-F, University of Michigan Research Institute, December, 1957.

19. Perez, S., "Cavitation Degree Measurements by Radioactive Attenuation," Term Paper, NE-299, Nuclear Engineering Department, University of Michigan, January, 1960.

20. Ripken, J. F. and J. M. Killen, "A Study of the Influence of Gas Nuclei on Scale Effects and Acoustic Noise for Incipient Cavitation in a Water Tunnel," St. Anthony Falls Hydraulic Laboratory, University of Minnesota, September, 1959.

21. Knapp, R. T., "Recent Investigations of the Mechanics of Cavitation and Cavitation Damage," Trans. ASME, October, 1955.

NOMENCLATURE

ρ_v = vapor density

ρ_l = liquid density

T = temperature

H = head

h_{fg} = latent heat of vaporization

N = count rate

A = cross-sectional area

D = diameter

G = volumetric flow rate

$\dot{m}$ = mass flow rate

P = pressure

g_c = conversion factor numerically equal to acceleration of gravity on earth's surface

APPENDIX

1. Derivation of "Method A" Reduction of Pitot-Tube Measurements

From the Pitot-tube measurements, one can convert local total and static pressure measurements into local velocity measurements of the fluid, (see following sections), giving a plot of local velocity vs radial position (see Figures 10 through 15).

Since it has been observed by experiment that there exists a water jet, surrounded by its vapor, in the diffuser, one may estimate the jet diameter by taking a representative mean velocity of the central portion (where the velocity profile is very flat), and thus calculate the approximate jet diameter from the known volumetric flow rate.

Let the volumetric flow rate be G (the data of Figures 10 through 15 were taken with $G = 54$ GPM), and the mean velocity at a particular axial position be v_m, the corresponding cross-sectional area be A_m. From continuity:

$$A_j = G/v_m$$

where A_j is the area of the jet.

The "void fraction" is them:

$$\text{Void } \% = \frac{A_m - A_j}{A_m}$$

In Table I, v_m is taken as the velocity near the centerline. This certainly gives a smaller A_j and consequently a larger void fraction than actually exists.

TABLE I

JET DIAMETER AND VOID FRACTION MEASUREMENTS

I. Diameter of Water Jets

Tap No.	Cold Water C	E	G	H	J	E(Hot Water)
0 cav.	0.503"	0.603"	0.750"	0.960"	1.17"	0.603"
1st mark cav.	0.459"	0.477"	0.501"	0.712"	0.948"	0.500"
2nd mark cav.	0.459"	0.477"	0.486"	0.486"	0.708"	0.500"
2-3/4 mark cav.	0.459"	0.477"	0.486"	0.500"	0.508"	0.500"

II. "Void" Fraction

Tap No.	Cold Water C	E	G	H	J	E(Hot Water)
0. cav.	0	0	0	0	0	0
1st mark cav.	0.174	0.33	0.56	0.448	0.117	0.265
2nd mark cav.	0.174	0.33	0.582	0.745	0.508	0.265
2-3/4 mark cav.	0.174	0.33	0.582	0.730	0.745	0.265

However, the choice of v_m does not seem too important since the velocity near the edge of the jet computed in this manner is still about 90 percent of v_{max}. Thus the percent of error due to inadequate choice of v_m should be tolerable.

2. Derivation of "Method B" Reduction of Pitot-Tube Measurements

If the various irreversibilities and the end effect in a Pitot-tube are negligible, the local stream velocity can be calculated by:

$$v = \sqrt{\frac{2g_c\Delta P}{\rho}} \qquad (1)$$

where v = fluid velocity
ΔP = pressure difference as measured by Pitot-tube
ρ = fluid density

Unfortunately, in a cavitating venturi, the density term ρ in Equation (1) is an unknown due to the presence of gas bubbles. These bubbles, at least locally, increase the bulk volume of the fluid. Thus, the velocity of the mixture, corresponding to a given velocity pressure, is increased. This is obvious from Equation (1), where ρ is definitely smaller than the actual density of the liquid, ρ_l.

Let the velocity v_m be defined as:

$$v_m = \sqrt{\frac{2g_c\Delta P}{\rho_l}} \qquad (2)$$

in which ΔP is measured by the Pitot-tube in the cavitating venturi. This velocity would equal the actual velocity if cavitation were not present. The volumetric flow rate, calculated by using Equation (2) is:

$$G' = \int_0^a 2\pi r v_m dr \tag{3}$$

while the actual volumetric flow rate is:

$$G = \int_0^a 2\pi r v dr \tag{4}$$

So the mass flow rate is given by:

$$\dot{m} = \int_0^a \rho\, 2\pi r v dr \tag{5}$$

In the above equation, "a" is the radius of the venturi at a given axial position. Combining Equation (1) and Equation (5), one obtains:

$$\begin{aligned} \dot{m} &= \int_0^a \rho \cdot 2\pi r v dr = \int_0^a \rho \cdot 2\pi r \sqrt{\frac{2g_c\Delta P}{\rho}}\, dr \\ &= \int_0^a \rho^{\frac{1}{2}} \cdot \rho_1^{\frac{1}{2}} 2\pi r \sqrt{\frac{2g_c\Delta P}{\rho_1}}\, dr = \rho_1^{\frac{1}{2}} \int_0^a \rho^{\frac{1}{2}}\, 2\pi r v_m dr \end{aligned} \tag{6}$$

If some mean value of ρ, $\bar{\rho}$, is used, Equation (6) becomes:

$$\dot{m} = (\rho_1 \bar{\rho})^{\frac{1}{2}} \int_0^a 2\pi r v_m dr = (\rho_1 \bar{\rho})^{\frac{1}{2}} G'$$

Therefore:

$$\dot{m} = \rho_1 G = (\rho_1 \bar{\rho})^{\frac{1}{2}} G'$$

or:

$$\bar{\rho} = \left(\frac{G}{G'}\right)^2 \rho_1$$

Consider the mass balance through a plane normal to the axis:

$$(G_l + G_v)\,\bar{\rho} = G_l\rho_l + G_v\rho_v \tag{8}$$

where G_l and G_v are volumetric flow rates of liquid and vapor across the same section, respectively. One obtains from Equation (8) the following relation:

$$\frac{G_l}{G_v} = \frac{\rho_l - \bar{\rho}}{\bar{\rho} - \rho_l} \tag{9}$$

The "void fraction" is defined as below, if it is assumed that there is no "slippage" between vapor and liquid.

$$\text{void } \% = \frac{G_v}{G_l + G_v} = \frac{1}{\frac{G_l}{G_v} + 1} = \frac{1}{\frac{\rho_l - \rho}{\bar{\rho} - \rho_l} + 1}$$

$$= \frac{\rho_l - \bar{\rho}}{\rho_l - \rho_v} \tag{10}$$

Combining Equations (7) and (10) and assuming $\rho_v \ll \rho_l$, one obtains

$$\text{void } \% = 1 - (G/G')^2 \tag{11}$$

It has been observed from the high-speed motion pictures, the evidence of previous investigations[1, 2], and theoretical reasoning given in the report that the vapor phase is concentrated along the wall and a water jet occupies the core. With the assistance of Equation (11), the approximate diameter of the water jet D_j can be

calculated; i.e.

$$\text{void } \% = \frac{\text{Area of the flow section - Area of the water jet}}{\text{Area of the flow section}}$$

$$= \frac{D^2 - D_j^2}{D^2} = 1 - \left(\frac{D_j}{D}\right)^2$$

$$\therefore D_j = D\left(\frac{G}{G'}\right)$$

where D = the diameter of the venturi at some section
D_j = the diameter of the center water jet
G' = the "psuedo flow rate" defined in Equation (3)
G = the actual flow rate

3. Derivation of "Method C" Reduction of Pitot-Tube Measurements

As stated in the text, a condensation shock could be formed in front of the Pitot needle. The momentum balance cross the shock wave, assuming a normal shock,

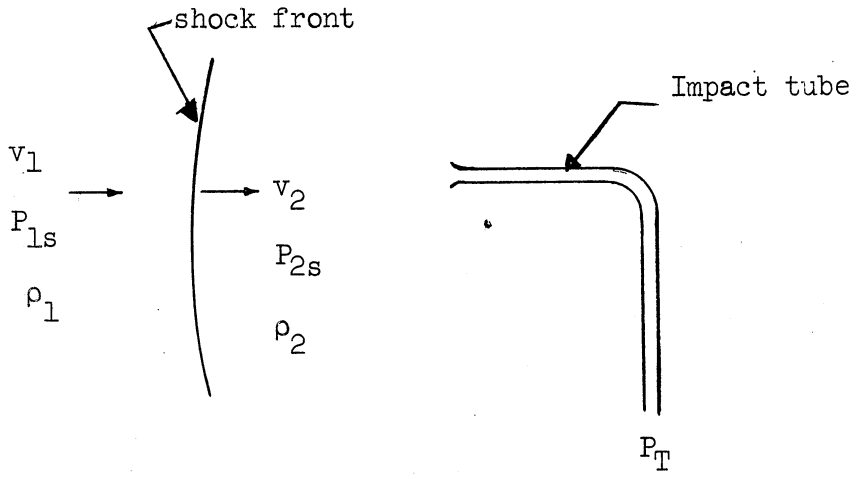

gives:

$$P_{2s} - P_{1s} = \frac{\dot{m}}{Ag_c}(v_1 - v_2) \qquad (12)$$

The continuity relation is:

$$\rho_1 v_1 = \rho_2 v_2 \tag{13}$$

Behind the shock wave, the pitot tube equation gives:

$$v_2 = \sqrt{\frac{2(P_{1s}-P_{2s})}{g_c \rho_2}} \tag{14}$$

If P_{2s} is measured, one can calculate a correction factor to take care of the shock effect using these relations. However, this measurement has not yet been accomplished.

4. Derivation of Jet Diameter from Gamma-Ray Void Fraction Measurements

As discussed in the text, the ratio of fluid path to total path in the test section for the source gamma-rays is given by:

$$X = \frac{N_{empty} - N_{actual}}{N_{empty} \quad N_{full}}$$

where N signifies count rate. Then:

$$1 - X = \frac{\text{Void Path}}{\text{Total Path}} = \frac{D - D\ jet}{D}$$

where D is test section diameter at points of interest.

The geometry of the source and counter apertures (Figure 23) is such that this procedure seems reasonable even though the beam is not closely correlated.